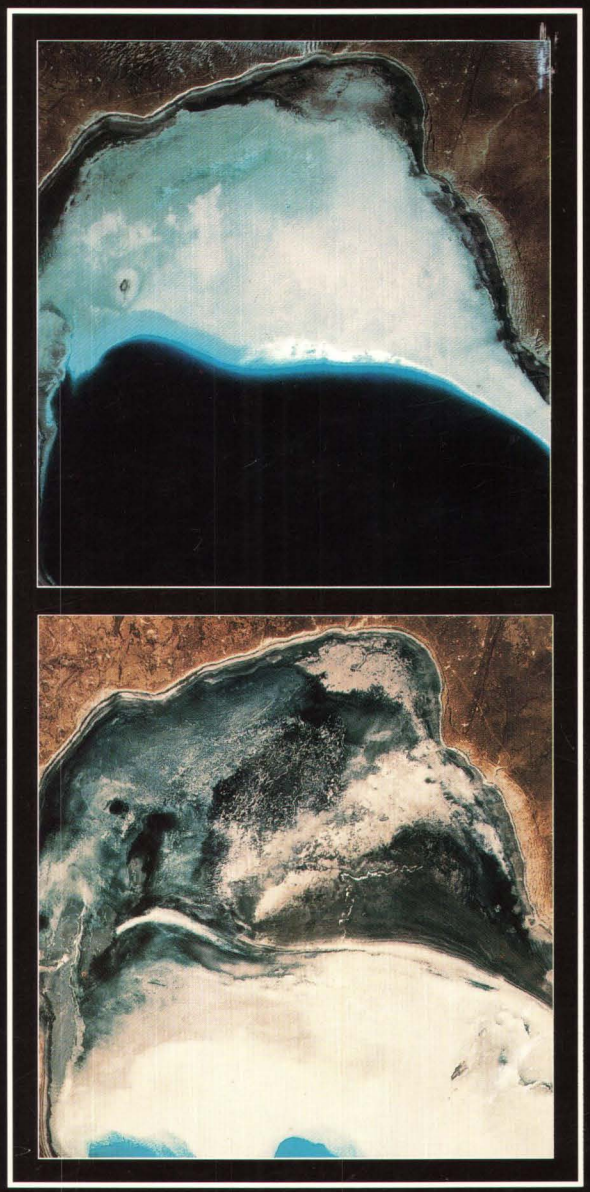

Historical Landsat
DATA COMPARISONS

• Illustrations of Land Surface Change •

U.S. Department of the Interior
U.S. Geological Survey

Historical Landsat Data Comparisons

Illustrations of Land Surface Change

Prepared by Matthew D. Cross

U.S. Department of the Interior
U.S. Geological Survey
EROS Data Center

Table of Contents

Introduction

The U.S. Geological Survey's (USGS) EROS Data Center (EDC) has archived two decades of Landsat data, providing a rich collection of information about the dynamics of the Earth's land surface. Major changes to the surface features of the planet can be detected, measured, and studied using Landsat data. The effects of desertification, deforestation, pollution, cataclysmic volcanic activity, and other natural and anthropogenic events can be examined by resource scientists using data acquired from the Landsat series of Earth-observing satellites. The availability of a nearly uninterrupted flow of information from the Landsats, in a consistent data format, gives researchers an important tool for studying surface changes over time.

This booklet provides an overview of the Landsat program and shows the application of the data to monitor changes occurring on the surface of the Earth. To show changes that have taken place within the last 20 years or less, image pairs were constructed from the Landsat multispectral scanner (MSS) and thematic mapper (TM) sensors. Landsat MSS data provide a historical global record of the land surface from the early 1970's to present. Landsat TM data provide land surface information from the early 1980's to present.

A Brief History of the Landsat Program

The Landsat system was developed by the National Aeronautics and Space Administration (NASA) to meet the needs of resource managers and earth scientists. The USGS assumed responsibility for data archiving and for distributing the data to the user community. On July 23, 1972, NASA launched the first in a series of satellites designed to provide repetitive global coverage of the Earth's land masses. Designated initially as Earth Resources Technology Satellite-A (ERTS-A), it used a Nimbus-type platform that was modified to carry sensor systems and data relay equipment. When operational orbit was achieved, it was designated ERTS-1.

The satellite was expected to last 1 year but continued to function beyond its designed life expectancy. It finally ceased to operate on January 10, 1978, almost 5 years after its launch date. The second in this series of Earth resources satellites (designated ERTS-B) was launched on January 22, 1975. It was renamed Landsat 2 by NASA and ERTS-1 was renamed Landsat 1. This was the official start of the Landsat program. Three additional Landsats were launched in 1978, 1982, and 1984 (Landsats 3, 4, and 5 respectively). Each successive satellite system had improved sensor and communications capabilities.

NASA was responsible for operating the Landsats through the early 1980's. In January 1983, operations of the Landsat system were transferred to the National Oceanic and Atmospheric Administration (NOAA). In October 1985, the Landsat system was commercialized and the Earth Observation Satellite Company assumed responsibility for its operation. Throughout these changes, the EDC retained primary responsibility as the U.S. Government archive of Landsat data. The EDC continues active research and development for Landsat data processing techniques to characterize and study changes on the land surface.

Characteristics of the Landsat System

Landsats 1 through 3 flew in a near-polar orbit at an altitude of 920 km with an 18-day repeat coverage cycle. It took 18 days and 215 overlapping orbits to provide near complete coverage of the Earth's surface with 185-km-wide image swaths. The amount of scene or swath overlap varied from 14 percent at the Equator to more than 60 percent in Alaska (fig. 1). The MSS sensor scans the Earth's surface from east to west as the spacecraft moves in its descending orbit over the sunlit side of the Earth. Six detectors for each spectral band provide six scan lines on each active scan. The combination of east-to-west sensor scan and north-to-south satellite movement generate the global coverage necessary for studying land surface change (fig. 2). The resolution of the MSS sensor is 57 m with radiometric coverage in four specified channels from the visible green to the near-infrared (IR) wavelengths (table 1). Only the MSS sensor onboard Landsat 3 had a fifth channel in the thermal-IR spectrum. Ground control at NOAA directs the specific areas to be scanned during the flight of the spacecraft.

Landsats 4 and 5 carry both the MSS and the TM sensors. They orbit at an altitude of 705 km and provide a 16-day, 233-orbit cycle with a swath overlap that varies from 7 percent at the Equator to nearly 84 percent at 80° north latitude. The fixed swath width is 185

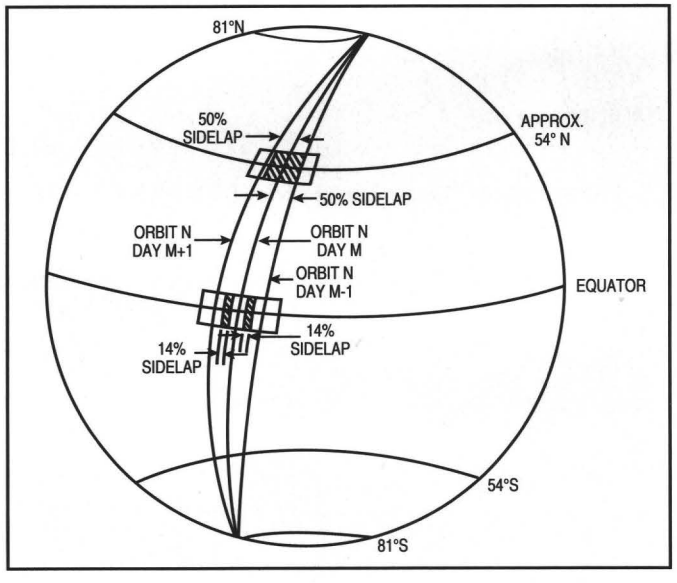

Figure 1. Orbital coverage of adjacent tracks of Landsats 1 through 3 (from Landsat Data Users Handbook, 1979, USGS).

Table 1

Radiometric range of channels for the MSS sensor (from Landsat Data Users Handbook, 1979, USGS).

Landsats 1 - 3	Landsats 4-5	Micrometers
4	1	0.5 - 0.6
5	2	0.6 - 0.7
6	3	0.7 - 0.8
7	4	0.8 - 1.1
8		10.4 - 12.6 (Landsat 3 only)

km (fig. 3). The MSS sensors aboard Landsats 4 and 5 are identical to the ones that were carried on Landsats 1 and 2. The MSS and TM sensors primarily detect reflected radiation from the Earth in visible and IR wavelengths, but the TM sensor provides more radiometric information than the MSS sensor. The wavelength range for the TM sensor is from visible blue, through the mid-IR spectrum, into thermal-IR (table 2). Sixteen detectors for the visible and mid-IR wavelength bands in the TM sensor provide 16 scan lines on each active scan. Four detectors for the thermal-IR band provide four scan lines on each active scan. The TM sensor has a spatial resolution of 30 m for the visible, near-IR, and mid-IR wavelengths and a spatial resolution of 120 m for the thermal-IR band. All of the Landsats have had a mid-morning equatorial crossing time.

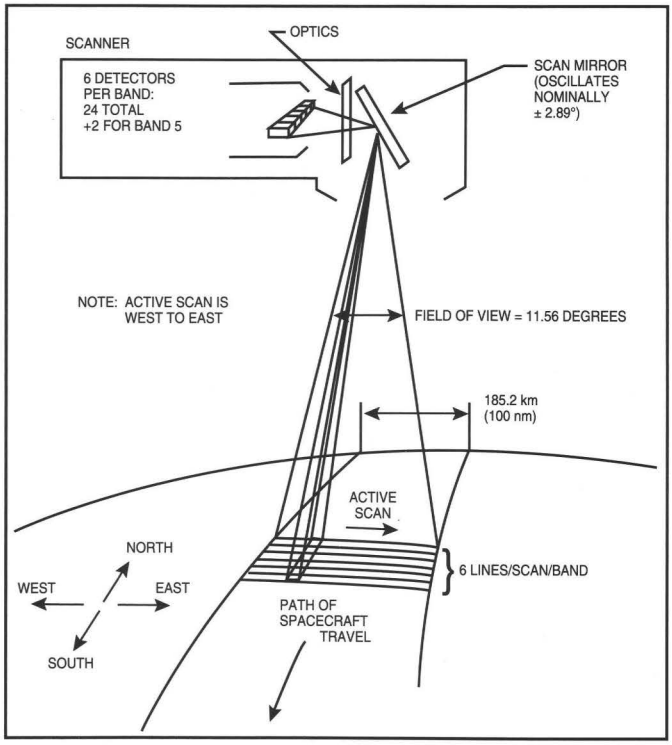

Figure 2 . Landsats 1 through 3 orbital tracks for 1 day of coverage (from Landsat Data Users Handbook, 1979, USGS).

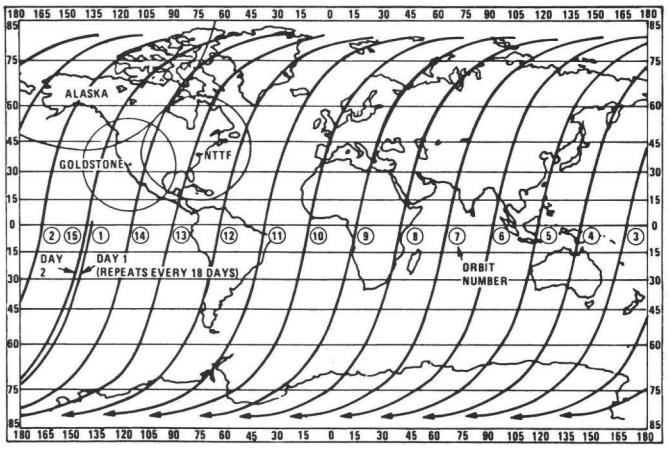

Figure 3. Orbital coverage of adjacent tracks for Landsats 4 and 5 (from Landsat 4 Data Users Handbook, 1984, USGS).

Table 2

Radiometric range of channels for the TM sensor (from Landsat 4 Data Users Handbook, 1984, USGS).

Landsat 4	Micrometers
1	0.45 - 0.52
2	0.52 - 0.60
3	0.63 - 0.69
4	0.76 - 0.90
5	1.55 - 1.75
6	2.08 - 2.35
7	10.40 - 12.50

Characteristics of Landsat Data

MSS and TM bands were chosen to maximize the sensing capabilities for detecting different types of land cover. For example, MSS band 1 is best for detecting green reflectance from healthy vegetation, and band 2 is best for detecting chlorophyll absorption. Bands 3 and 4 are best for near-IR emission peaks in healthy green vegetation. Bands 4, 2, and 1 can be combined to make a false-color composite image where band 4 represents red, band 2, green, and band 1, blue. This color image depicts water bodies as blue, sand and soil as tan or brown tones, and healthy vegetation as bright red. The same application can be performed with TM data using bands 4, 3, and 2 in red, green, and blue, respectively. The Landsat images in this publication are all false-color composite images. All of the images are from the MSS sensor onboard Landsats 1 through 5 except for the 1989 image for Yellowstone National Forest, which is a TM image. With the false-color composite technique described above, water bodies can be clearly delineated, clouds appear as bright white and can be easily identified, variations in soil can be observed, and healthy vegetation can be distinguished from vegetation under stress.

Landsat MSS and TM Applications

The Landsat data in this booklet show some of the dramatic changes that have taken place on the Earth in the last 20 years and demonstrate potential applications for monitoring the conditions of the Earth's land surface. The images have been paired to produce 15 examples of anthropogenic and natural changes on the Earth. The changes include agricultural development, deforestation, natural disasters, urbanization, and water resources. These images represent a small proportion of the Landsat data archive at the EDC that is available to the research community and the public.

Locator Map

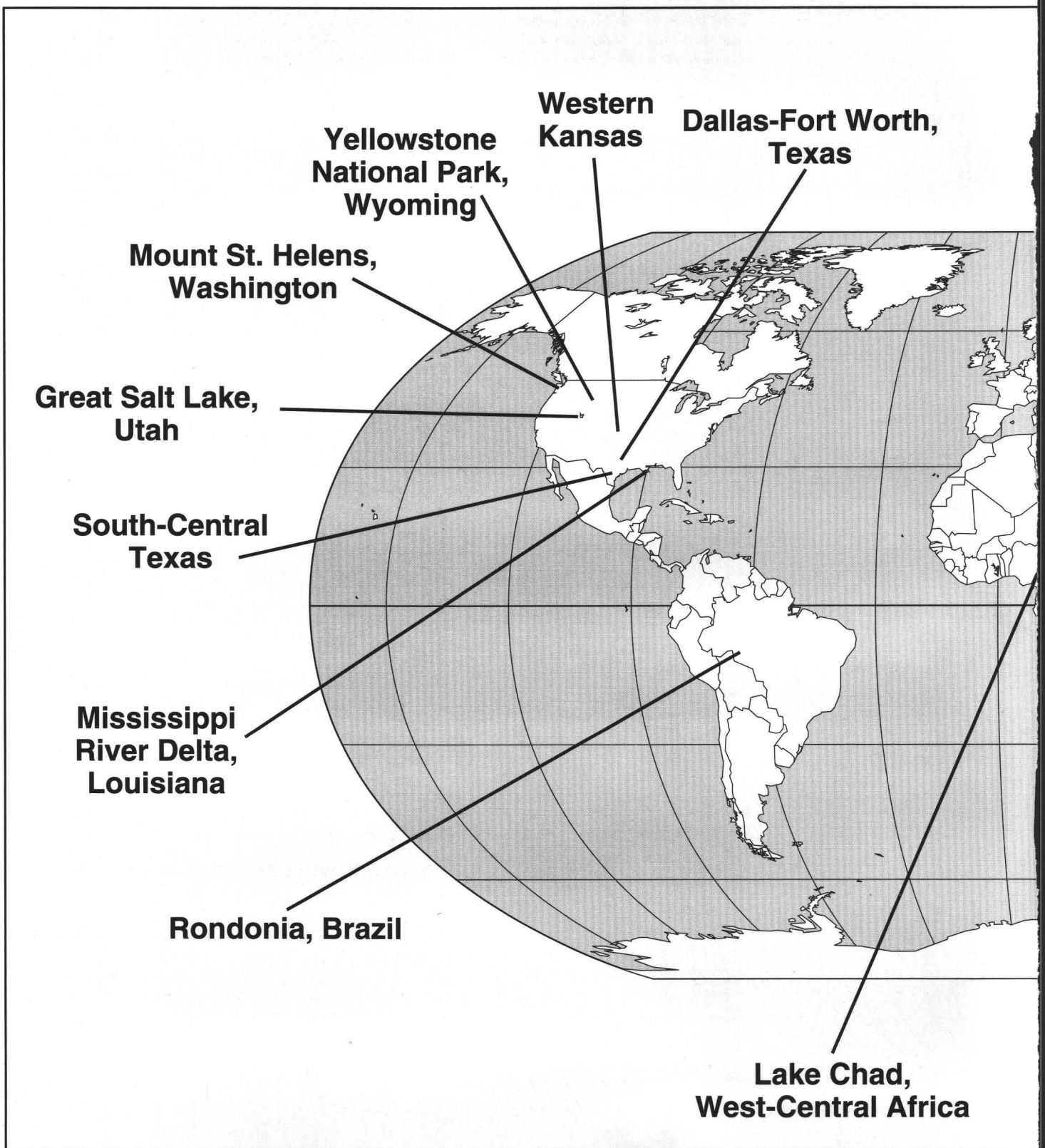
Western Kansas
Dallas-Fort Worth, Texas
Yellowstone National Park, Wyoming
Mount St. Helens, Washington
Great Salt Lake, Utah
South-Central Texas
Mississippi River Delta, Louisiana
Rondonia, Brazil
Lake Chad, West-Central Africa

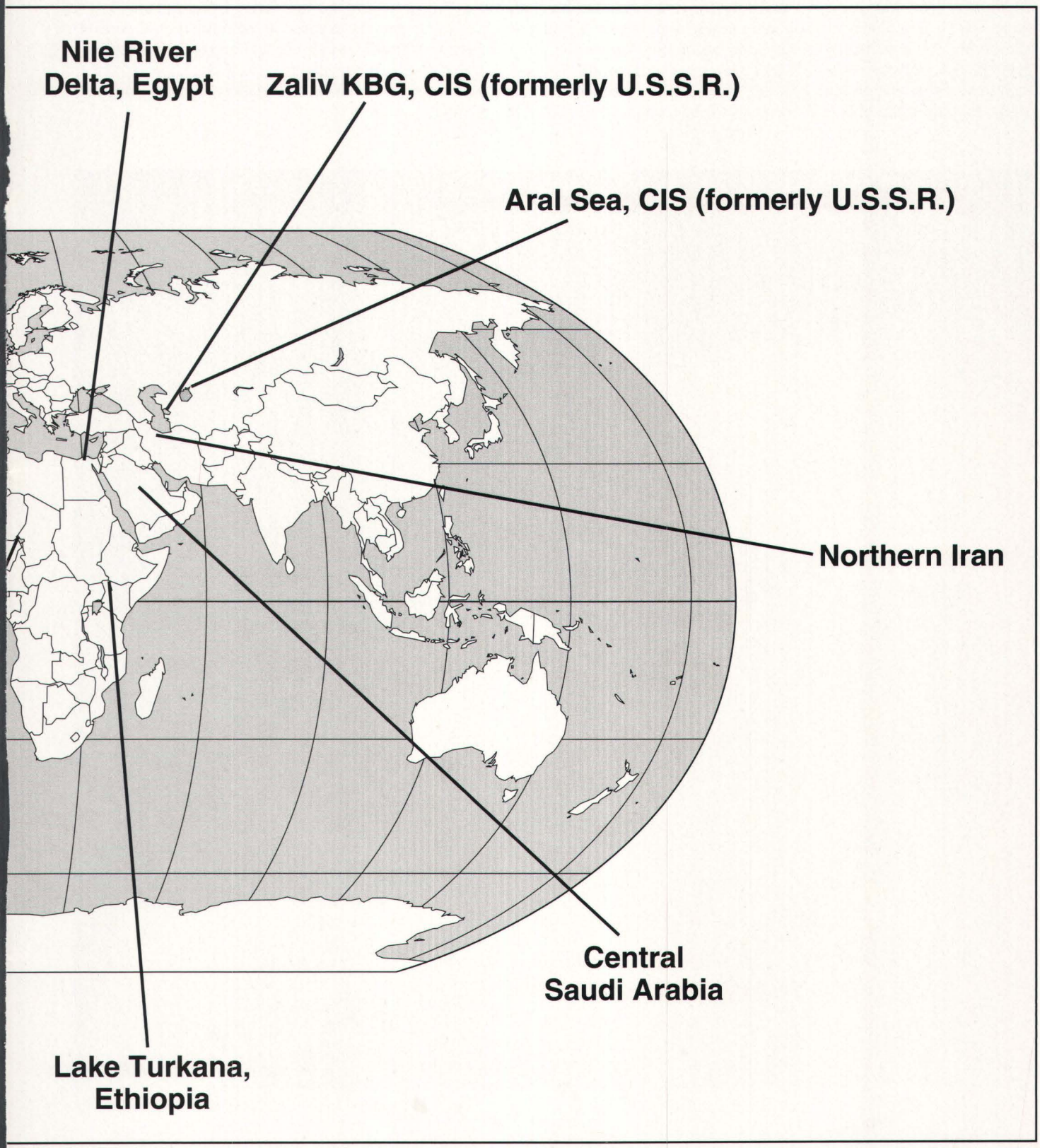
Nile River
Delta, Egypt
Zaliv KBG, CIS (formerly U.S.S.R.)
Aral Sea, CIS (formerly U.S.S.R.)
Northern Iran
Central
Saudi Arabia
Lake Turkana,
Ethiopia

Nile River Delta, Egypt

The images from May 10, 1973, and July 18, 1987, show the dramatic urban growth within the Nile River Delta and the expansion of agriculture into adjoining desert areas. Cairo, Egypt, (shown as the large gray expanse in the right-central portion of each image) dramatically increased in population, from 4.2 million in 1966 to 5.8 million in 1982, and currently has a population density of close to 70,000 people per square mile. The area of vegetation just outside the delta in the upper-left of each image is new agricultural development, with some of the crops irrigated through center-pivot irrigation. The development of this new agricultural land is because of urbanization of formerly farmed land.

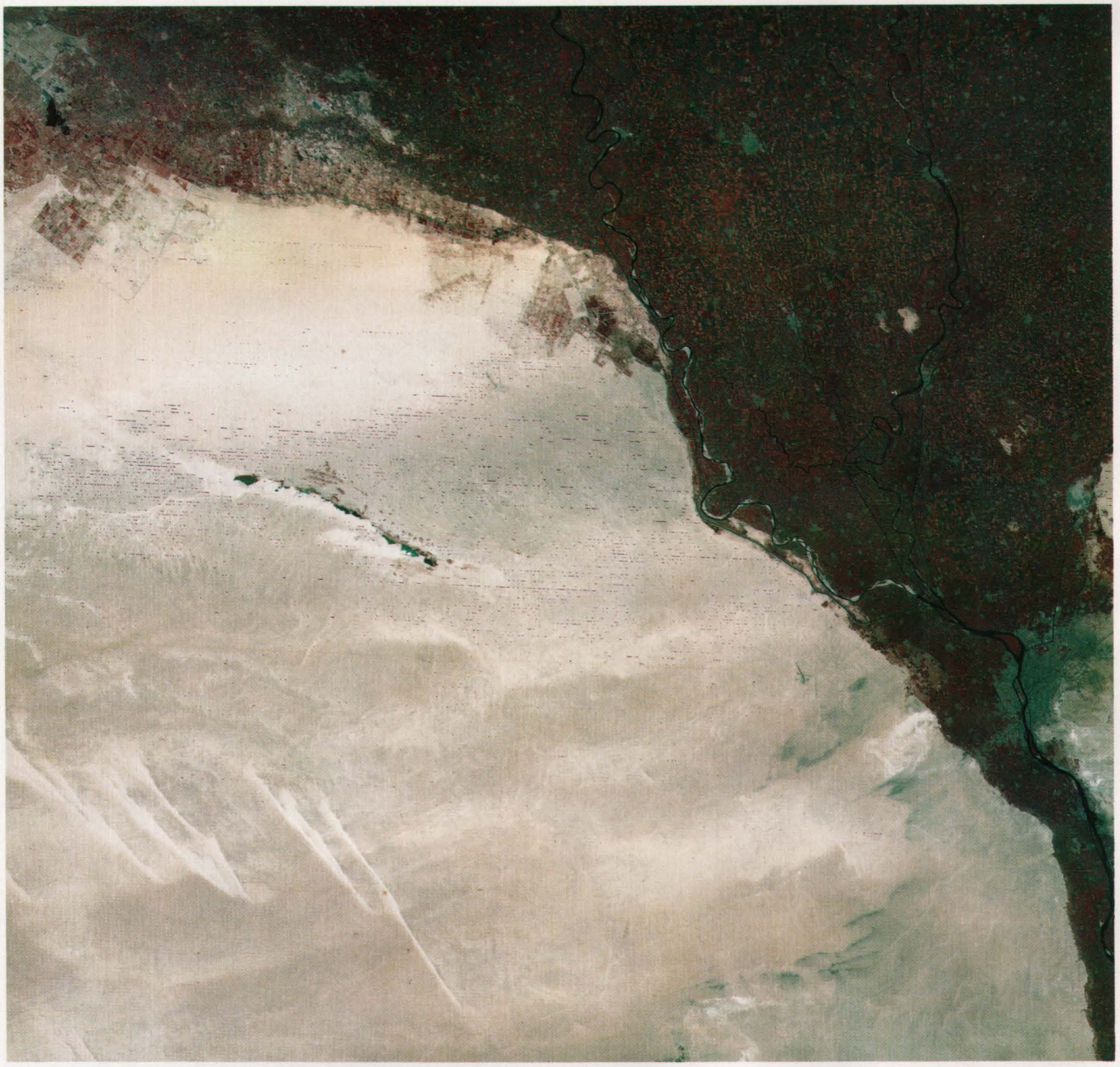

Landsat MSS
May 10, 1973

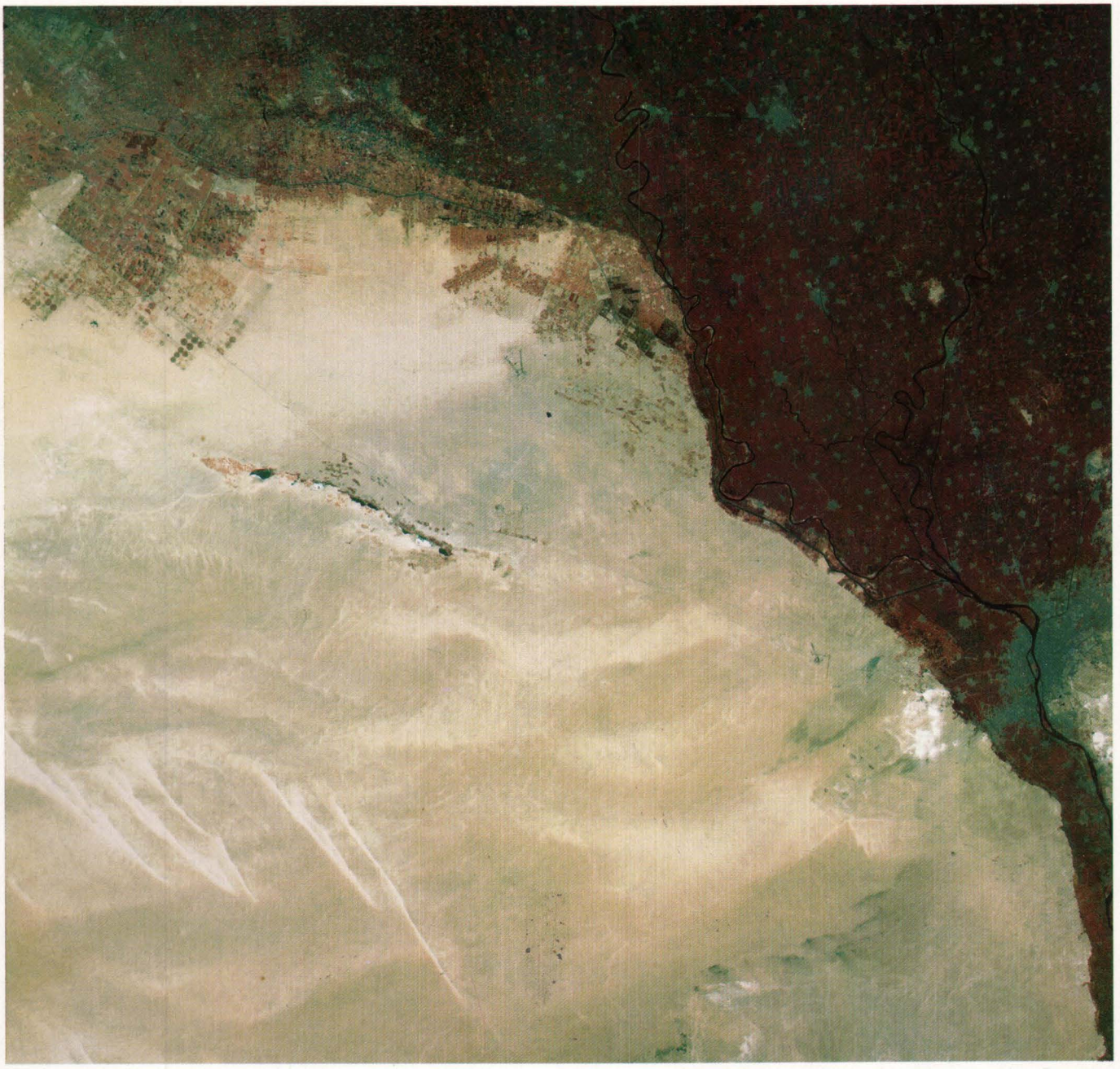

Landsat MSS
July 18, 1987

Center-Pivot Irrigation, Western Kansas

Much of the natural shortgrass prairie of the Kansas Sand Hills is now irrigated cropland. The number of center-pivot irrigation systems in Finney County, western Kansas, has increased dramatically since the early 1970's. The two August Landsat images show center-pivot irrigated crops as red circles. The predominant crop grown in this area of Kansas is corn. Light colored cultivated fields in the images are fallow or recently harvested. Irrigation is possible because of the fossil waters from the Ogallala aquifer, which ranges from Nebraska and Wyoming south to the Texas Panhandle. Landsat images such as these play a major role in providing an inventory of irrigated crop acreage, a key component of modeling aquifer response to changes in water use.

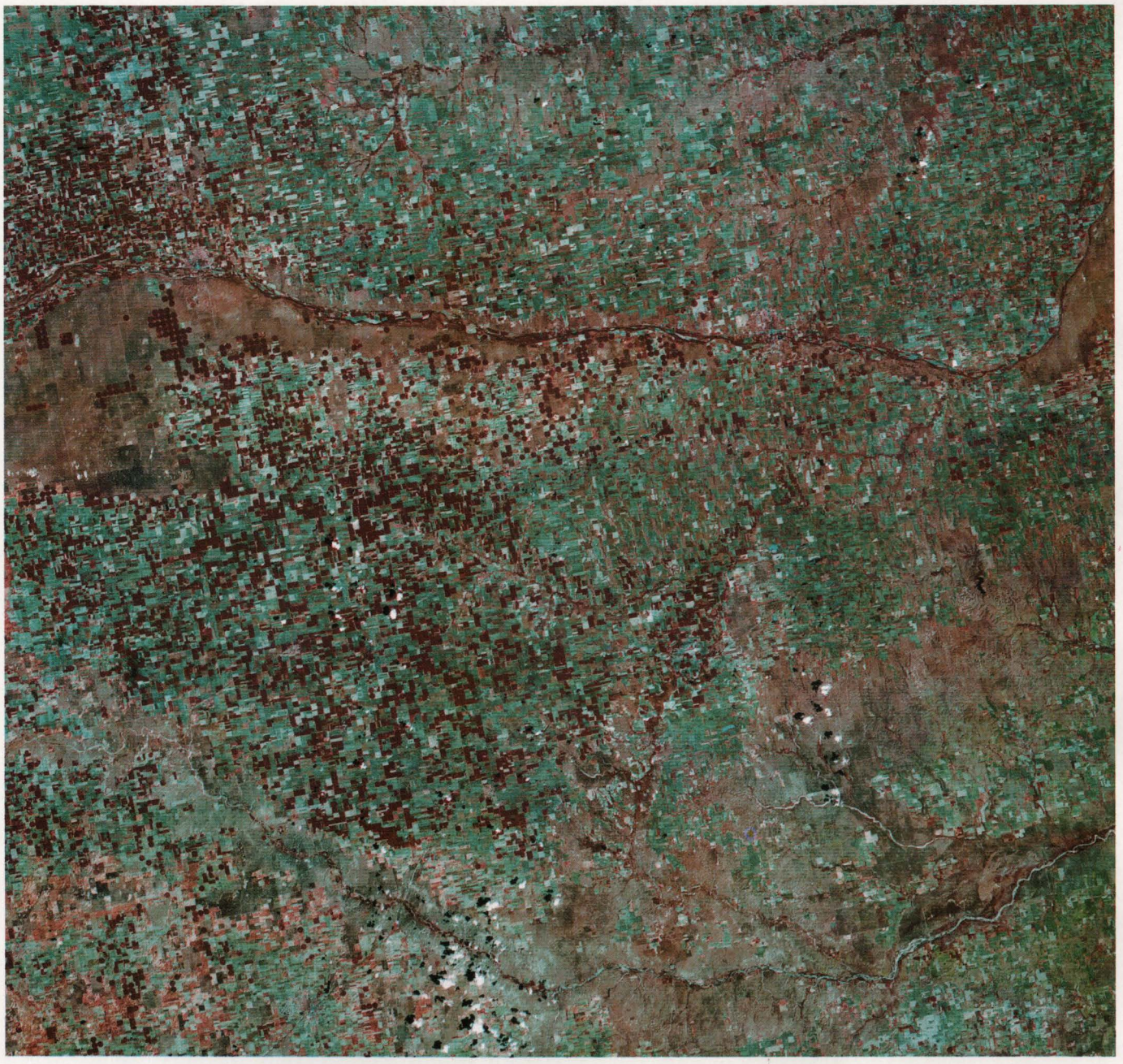

Landsat MSS
August 16, 1972

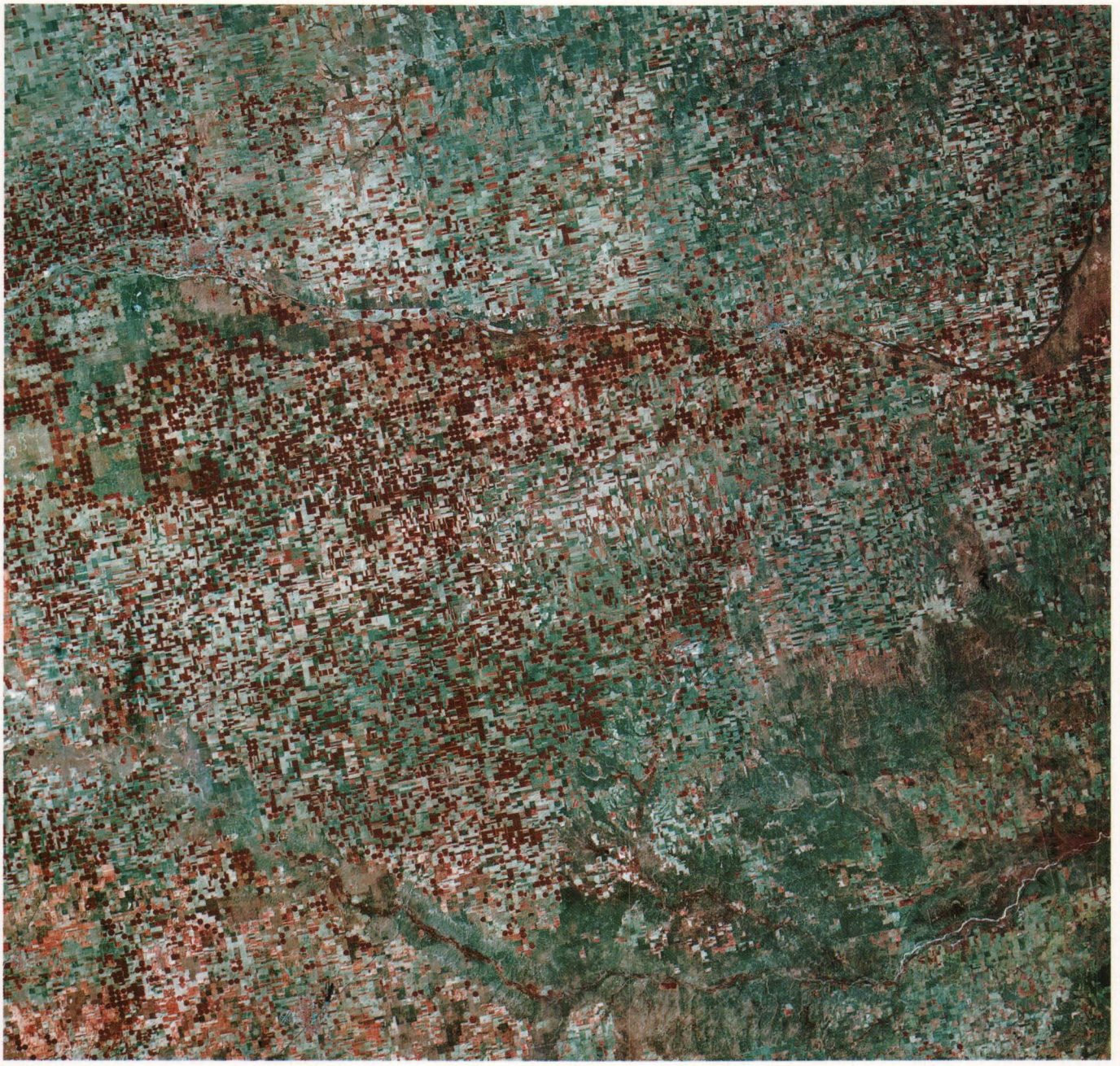

Landsat MSS
August 15, 1988

Northern Iran

Irrigated agriculture has increased in the valley south of the Elburz Mountains in Northern Iran (central part of each image) between July 14, 1977, and September 16, 1987. This mountain range parallels the Caspian Sea and acts as a barrier to rain clouds moving southward. A rain-shadow effect on the northern slopes of the Elburz Mountains supports a heavy rain forest where rainfall is plentiful (dark red area in the north-northeast part of each image). The valley to the south of the mountain range receives little or no rainfall, causing very arid conditions. Local farmers take advantage of this extreme imbalance in rainfall by creating channels that capture rainfall from the mountain range. These channels run to the valley floor, where they provide water for crop irrigation. Extensive diversion of nearby rivers and the drilling of wells also help provide water for irrigation in this arid valley.

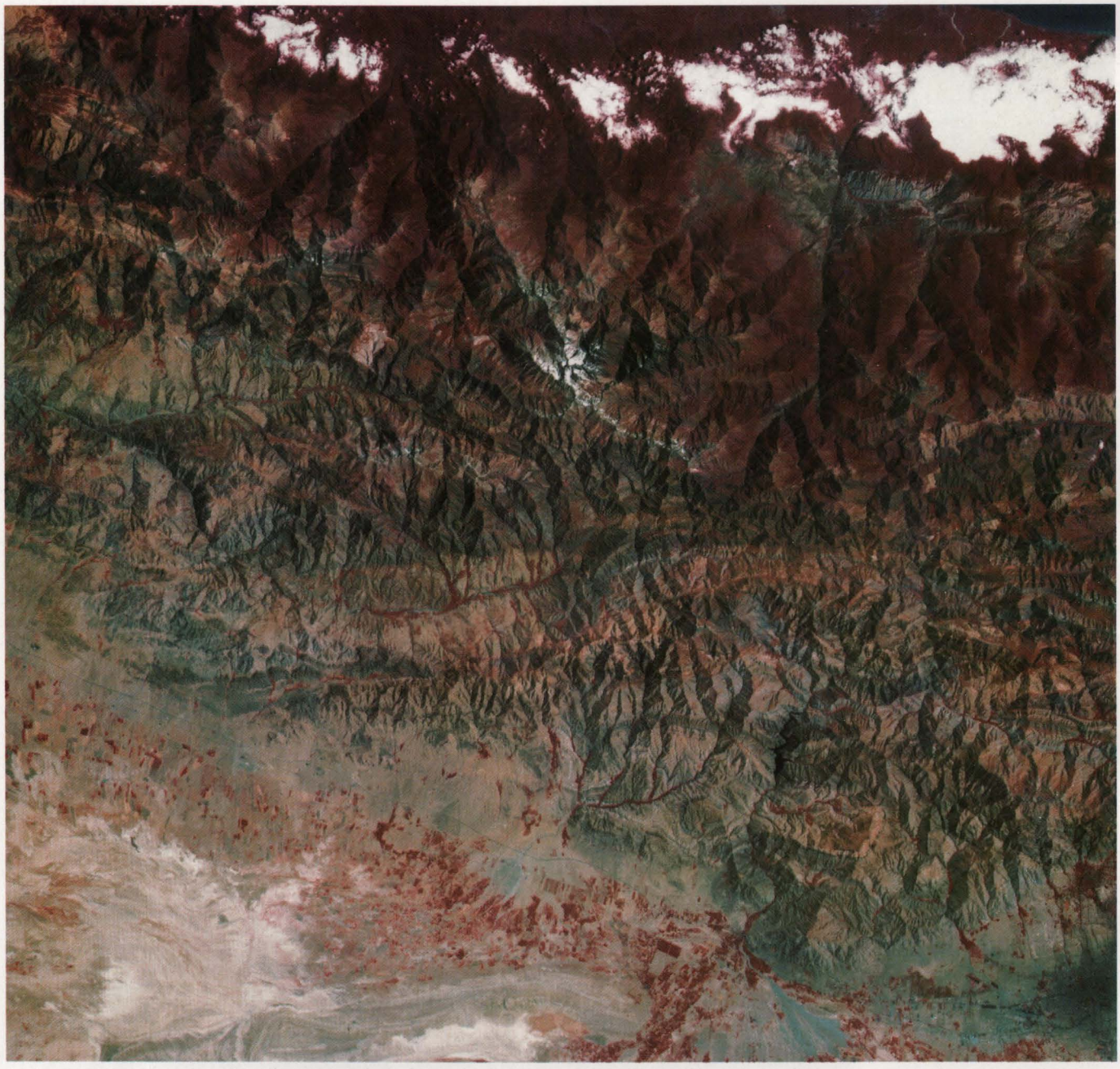

Landsat MSS
July 14, 1977

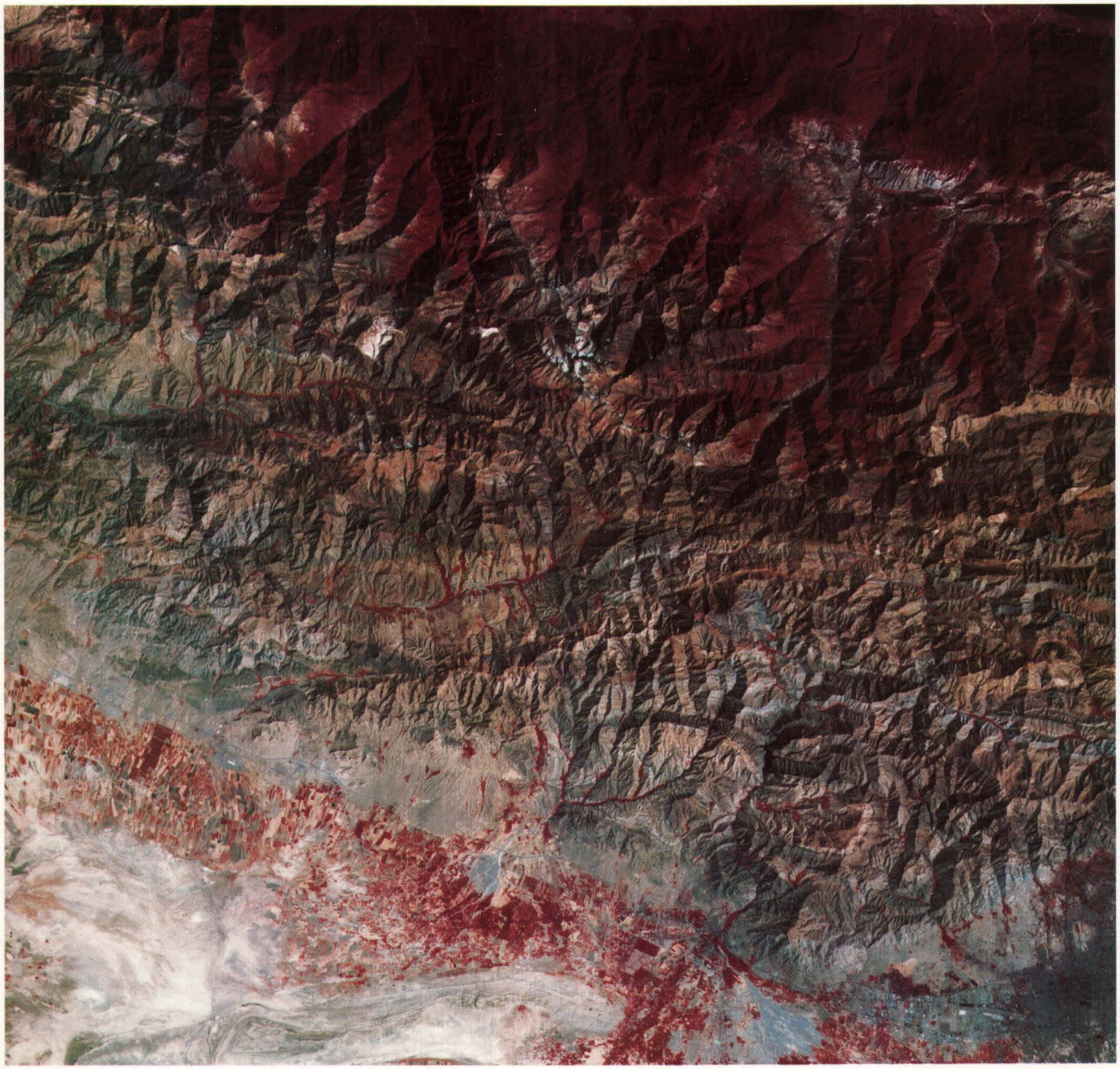

Landsat MSS
September 16, 1987

Center-Pivot Irrigation, Saudi Arabia

The development of center-pivot irrigation agriculture in Saudi Arabia is shown in the Landsat MSS scenes acquired on December 25, 1972, and February 15, 1986. There are no center-pivot irrigation systems in 1972, but hundreds had been developed by 1986. Center-pivot irrigation is identified by small red circles in the 1986 image. The predominant crop grown in this area is wheat. The scene includes the cities of Buraydah and Unayzah (northwest of Riyadh), Saudi Arabia. The new irrigation systems extend far beyond the images and cover a widespread area through central Saudi Arabia. Part of Saudi Arabia's oil revenues are directed toward agricultural development in an effort to modernize agricultural practices.

Landsat MSS
December 25, 1972

Landsat MSS
February 15, 1986

Rondonia, Brazil

These Landsat images show a portion of the state of Rondonia, Brazil, in which forest cutting has taken place from June 19, 1975, to August 1, 1986. Systematic cutting of the forest vegetation starts along roads and then fans out to create the "feather" pattern shown in the eastern half of the August 1, 1986, image. The cutover land and urban areas appear in light green and blue, whereas healthy vegetation is red.

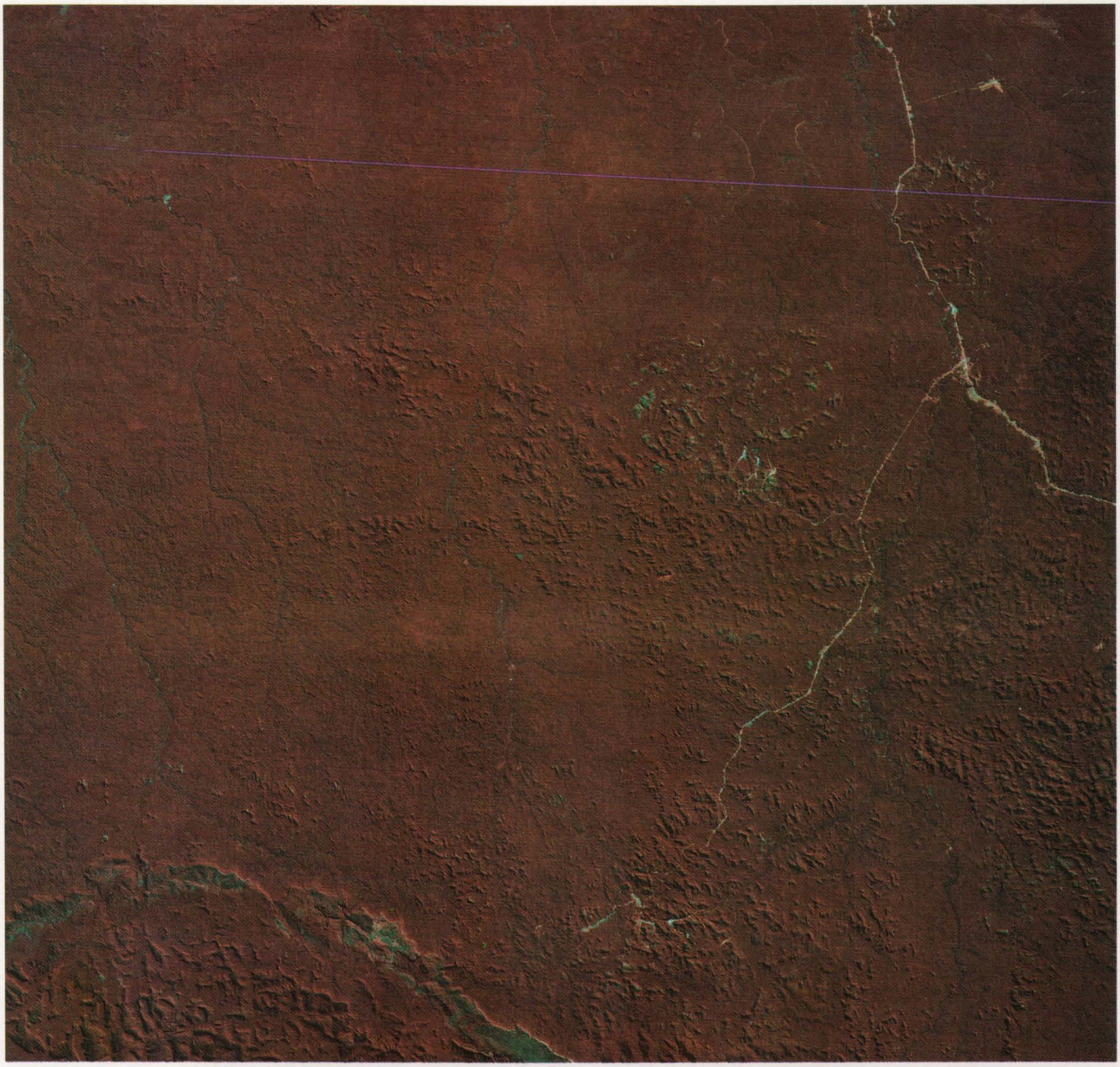

Landsat MSS
June 19, 1975

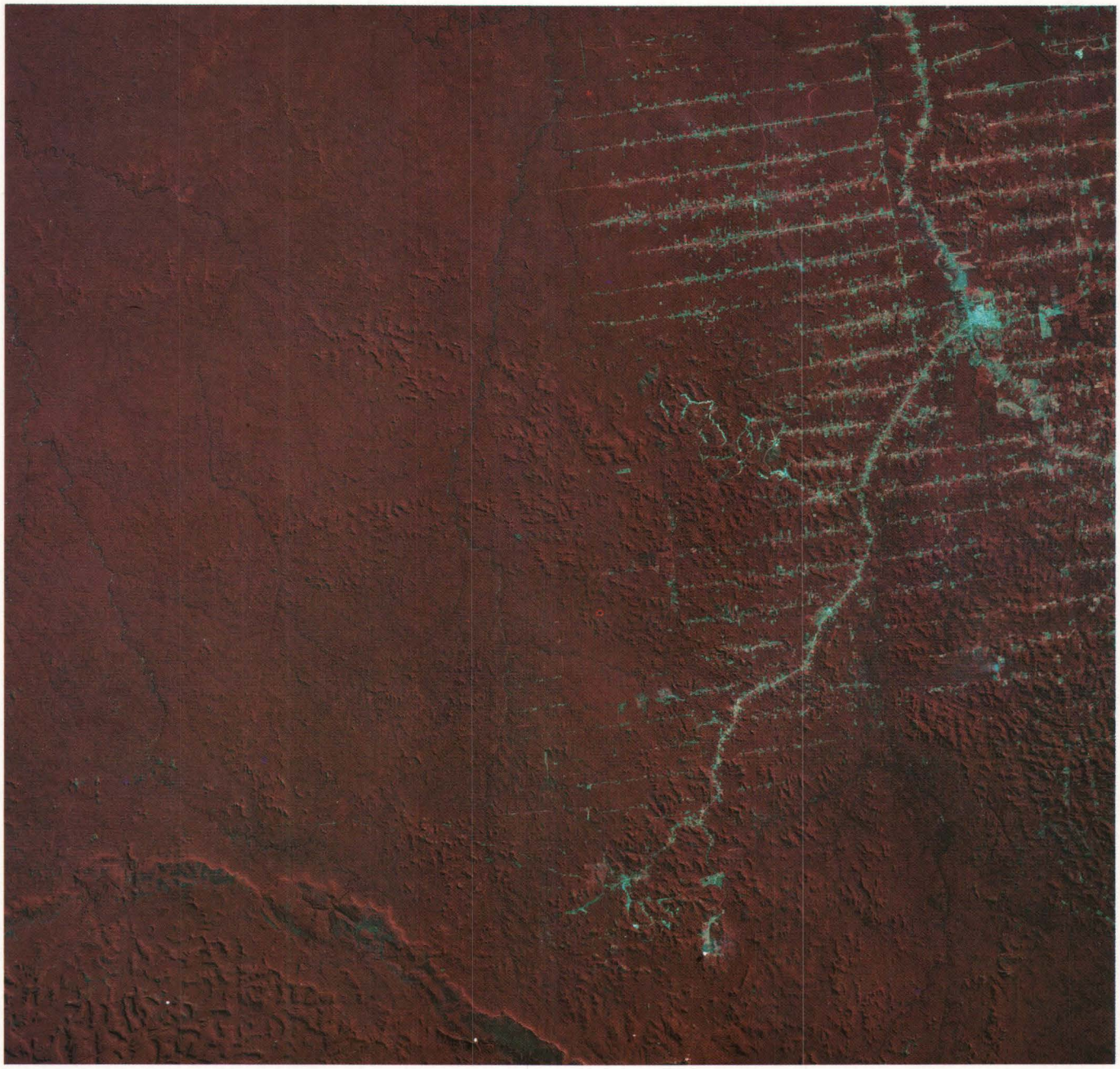

Landsat MSS
August 1, 1986

Mount St. Helens, Washington

Three Landsat images document the changes that have taken place in the vicinity of Mount St. Helens during the last 15 years. The September 15, 1973, image shows Mount St. Helens and adjacent forest land before the eruption on May 18, 1980. The May 22, 1983, image shows the areal extent of volcanic debris caused by the explosive eruption, with the collapsed north edge of the crater clearly evident. The area north of the crater is the most devastated with mud slides, volcanic ash, and mud-laden rivers shown as grayish-blue areas. Swift Reservoir, located to the south of the mountain, received silt and ash-laden runoff from the damaged areas.

The August 31, 1988, image shows some vegetation regrowth (light red and pink) in the destroyed area. The patchwork block patterns in the forested land east of Mount St. Helens are areas where timber has been removed. The August 31, 1988, image shows an increase in the amount of timber harvested from land in this region when compared with the September 15, 1973, image.

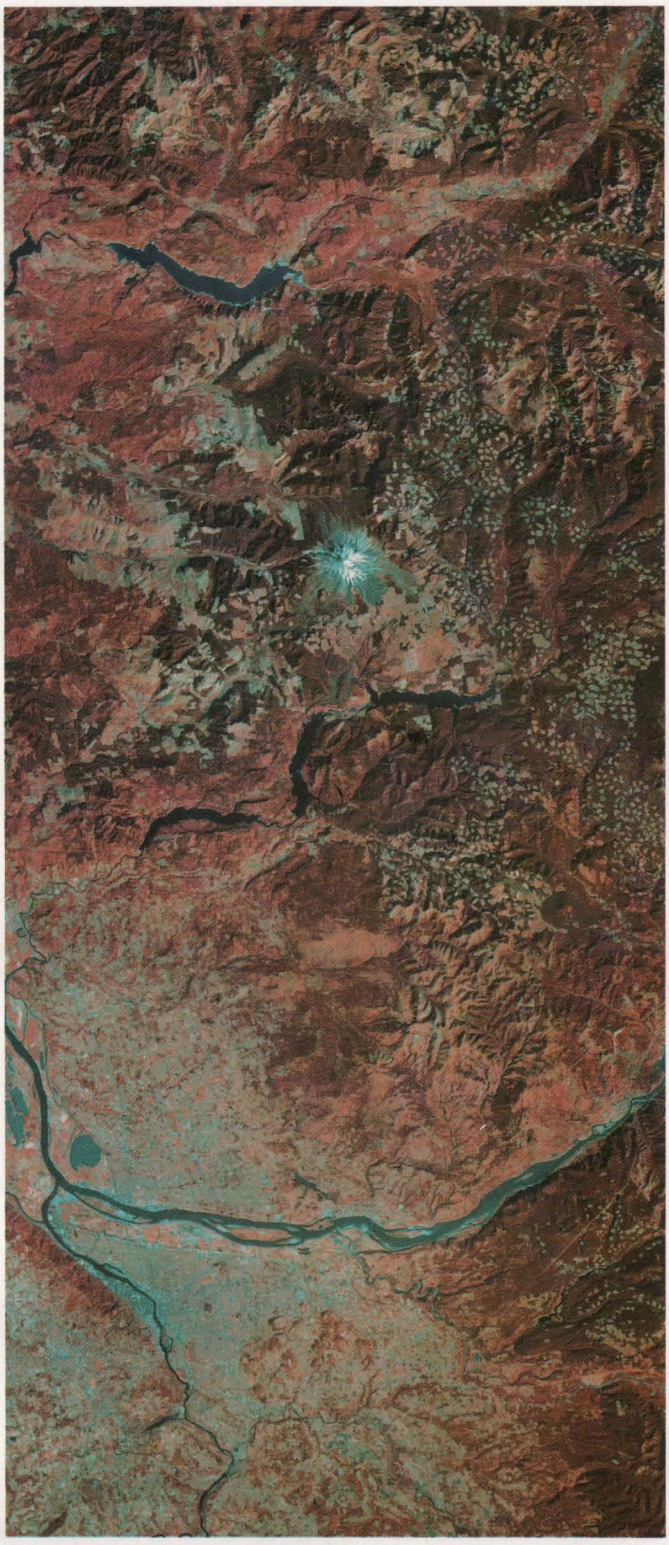

Landsat MSS
September 15, 1973

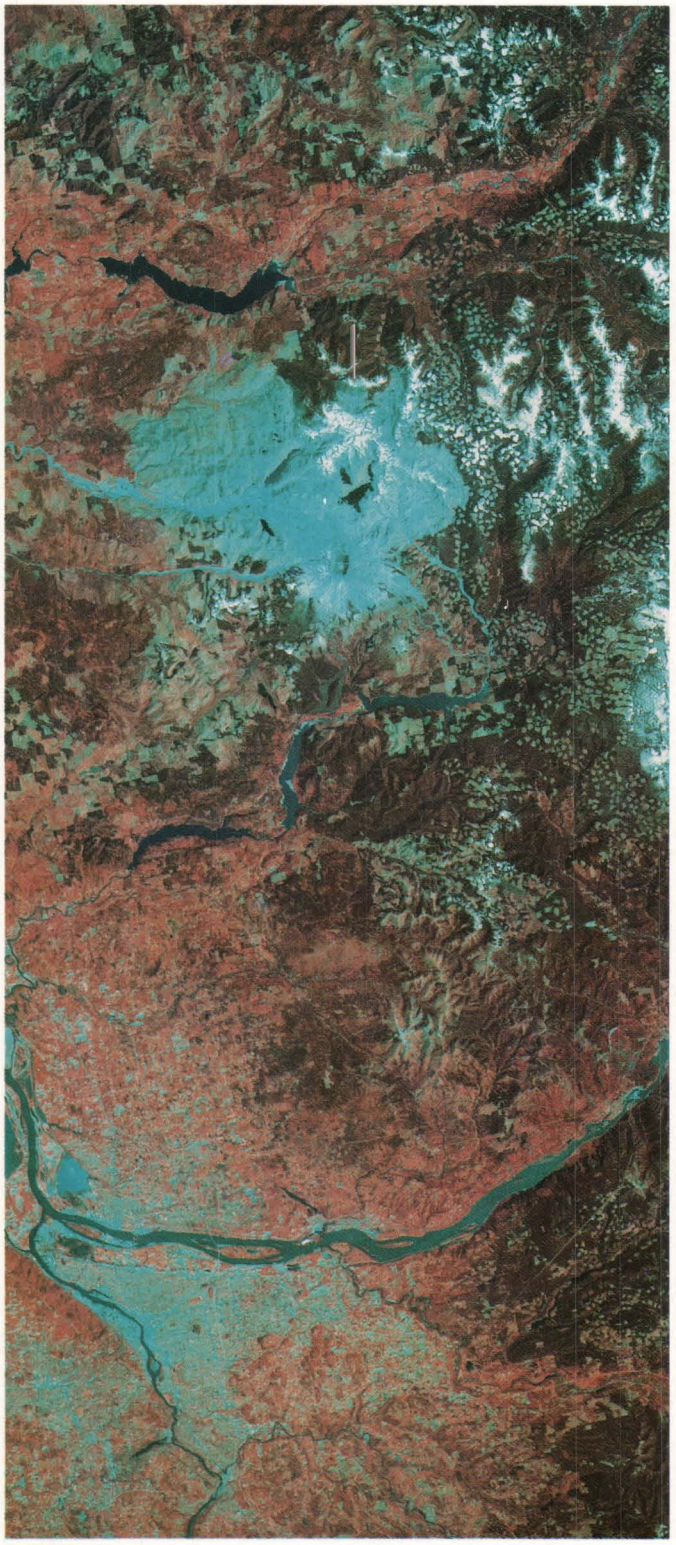

Landsat MSS
May 22, 1983

Landsat MSS
August 31, 1988

Yellowstone National Park, Wyoming

The Landsat MSS scene from August 4, 1972, and the Landsat TM scene from August 2, 1989, illustrate changes that have occurred in and adjacent to Yellowstone National Park during the 17-year period. The wildfires that occurred in the summer of 1988 can be seen as dark green to charcoal tones on the 1989 image. The boundary of the burned areas within Yellowstone National Park can be determined by comparing color tones between the two Landsat images. By delineating the burned lands, it is possible to monitor the successional changes occurring within the burned plant communities using subsequent Landsat images.

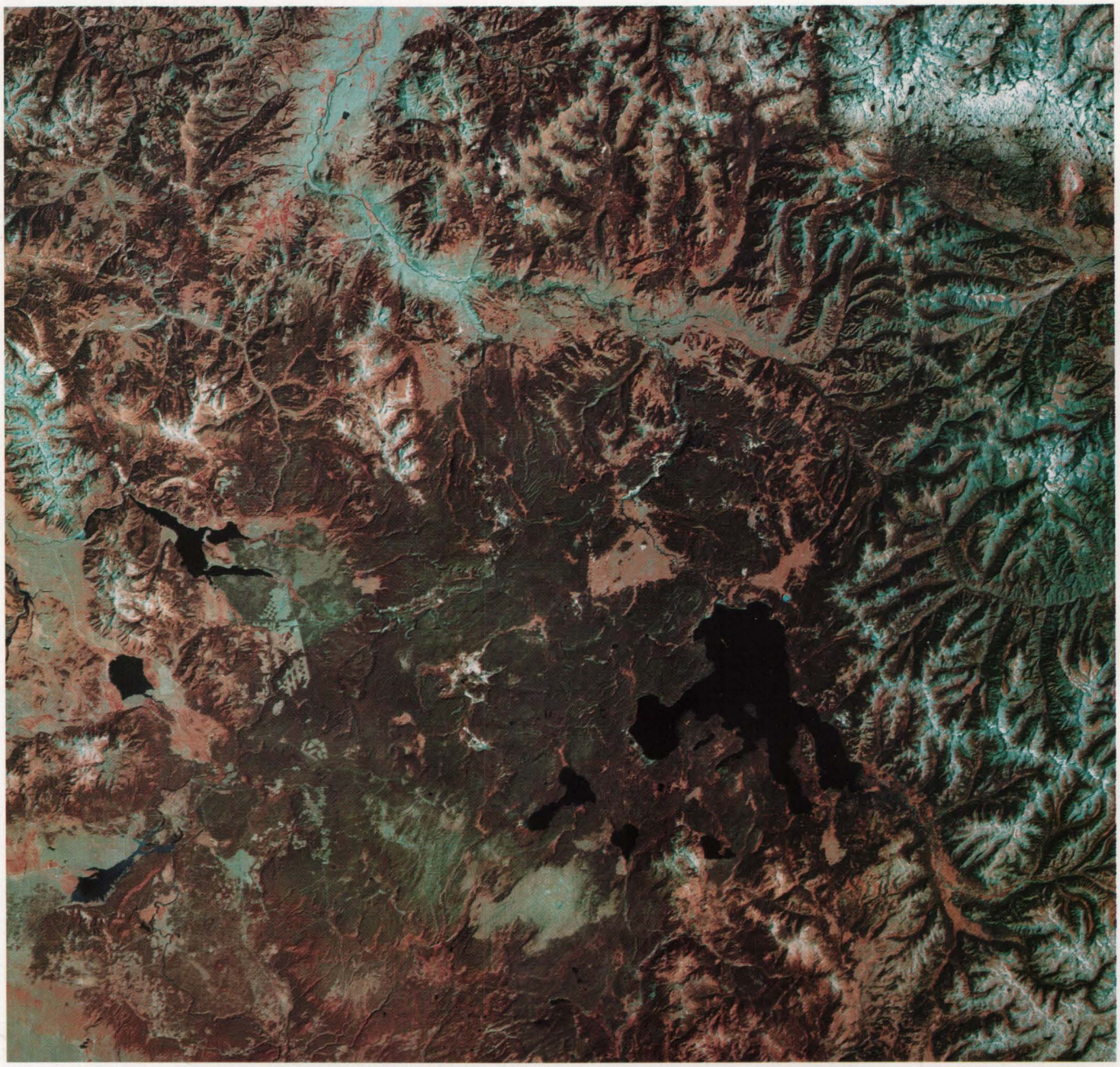

Landsat MSS
August 4, 1972

Timber harvesting is characterized by a patchwork pattern, seen along and outside the western edge of the park in the 1989 image. This pattern illustrates the differences in land management practices between park lands, where timber harvesting is prohibited, and on adjacent privately owned land and National Forest land, where timber harvesting is permitted.

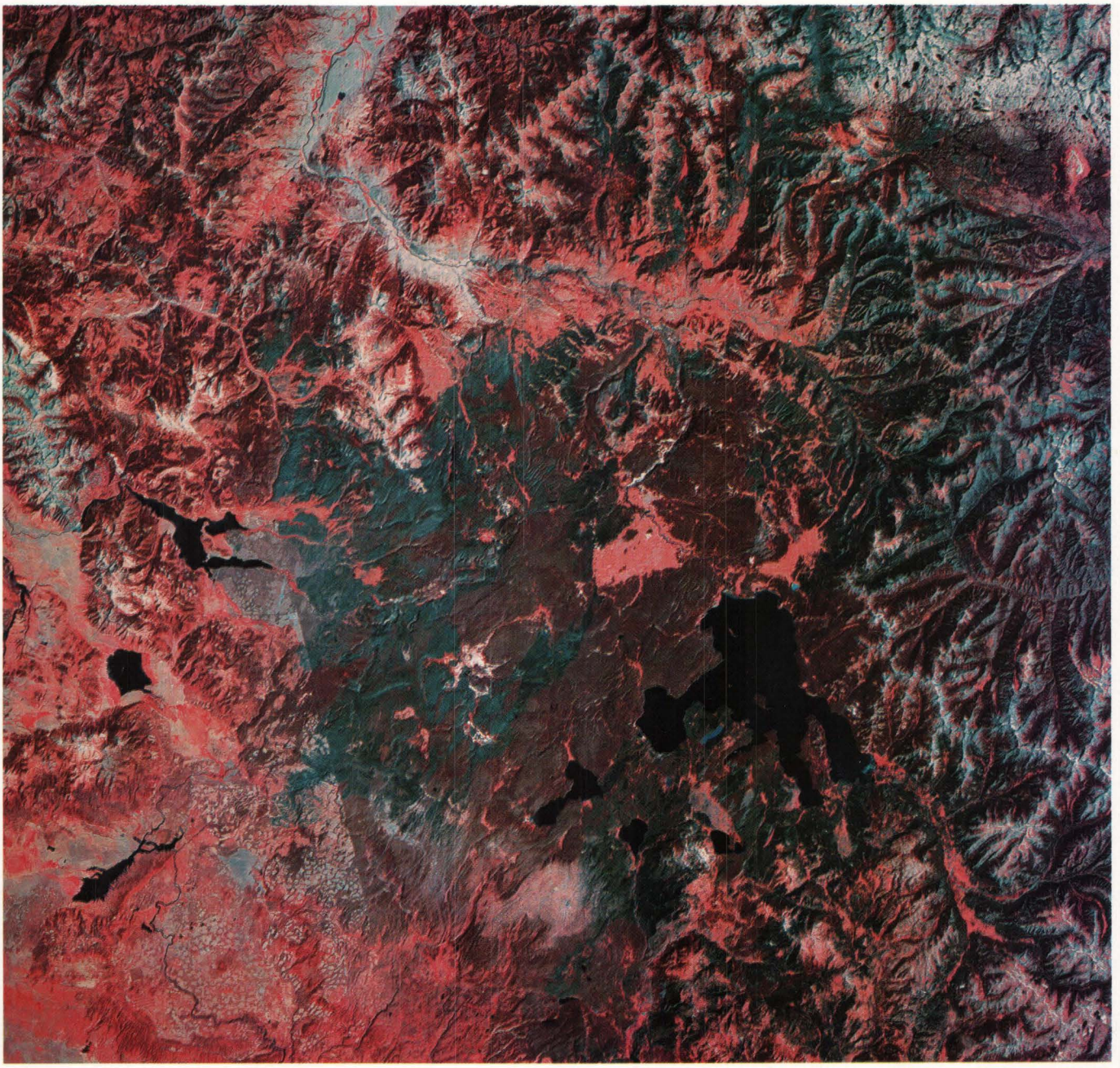

Landsat TM
August 2, 1989

Dallas-Fort Worth, Texas

The urban expansion of the Dallas-Fort Worth, Texas, area in the last 20 years is significant. The images acquired on March 12, 1974, and on March 22, 1989, show the expansion of urban areas into the surrounding countryside, replacing arable land. The population of this metropolitan area grew from 2,524,100 in 1974 to 3,776,000 by 1989. The new reservoir southwest of Dallas, and the expansion of Dallas-Fort Worth International Airport located between Dallas and Fort Worth, are apparent in the 1989 image.

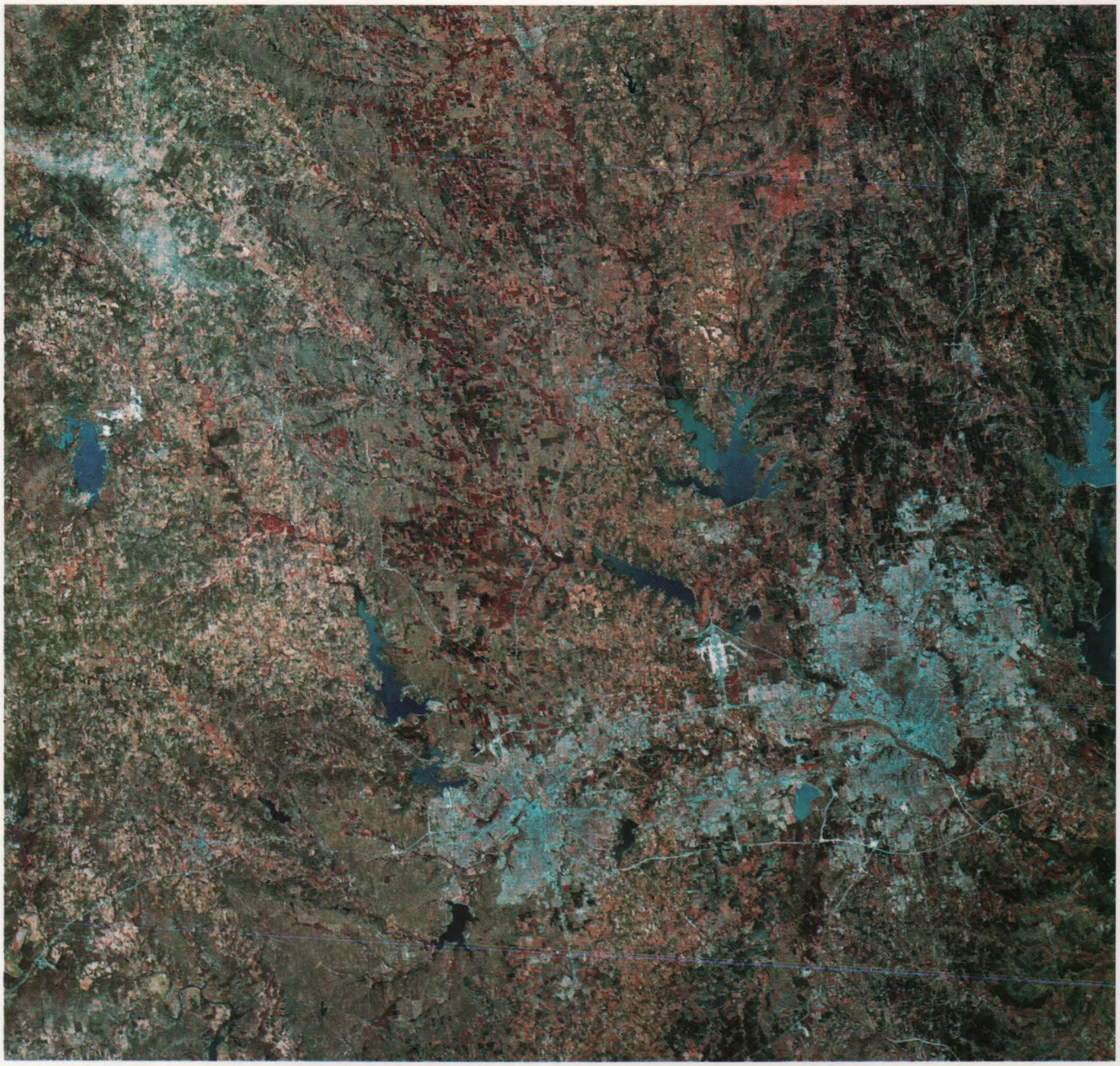

Landsat MSS
March 12, 1974

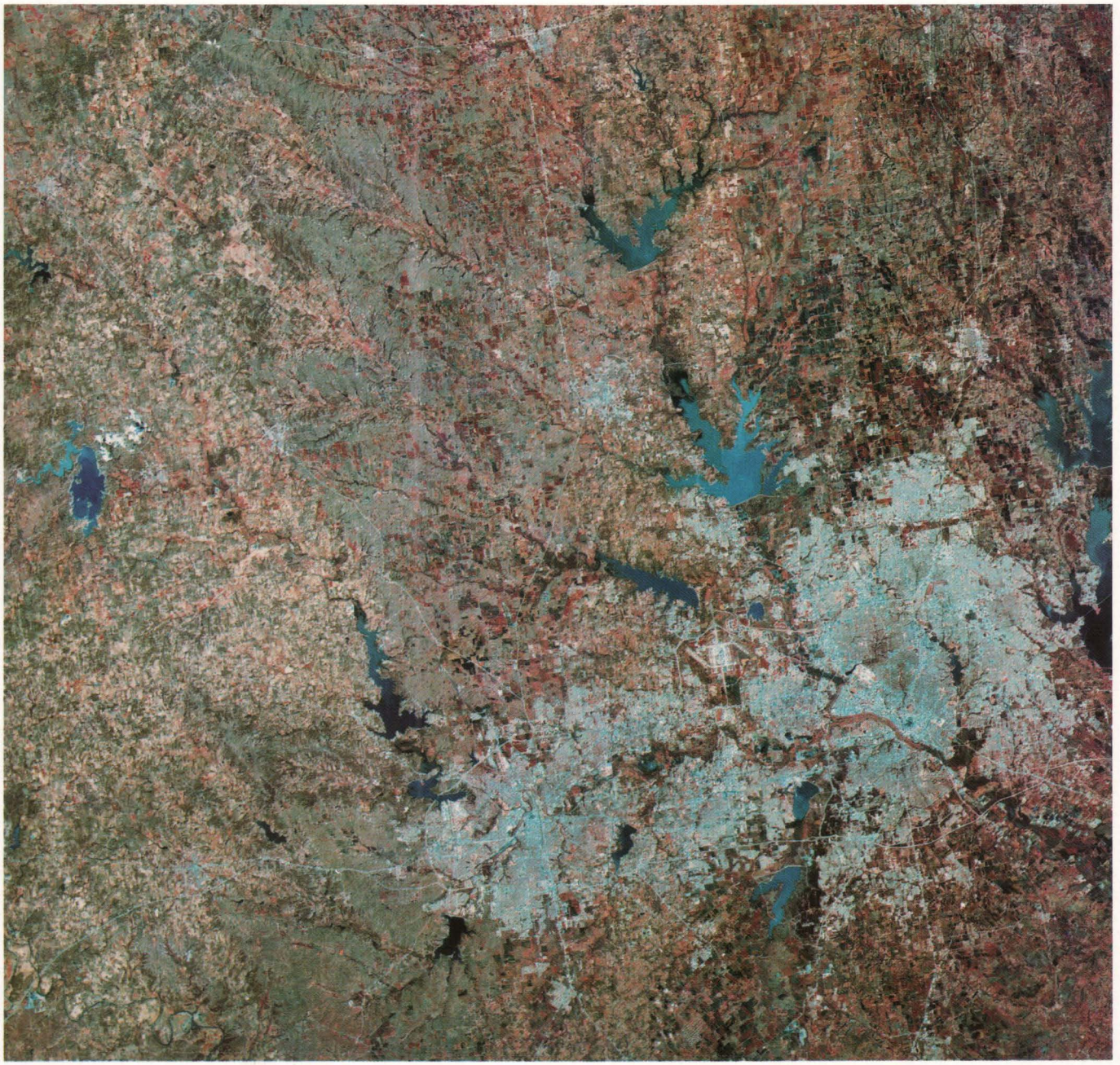

Landsat MSS
March 22, 1989

South-Central Texas

Images acquired over south-central Texas show the development of a new reservoir on the Nueces River between May 14, 1973, and June 1, 1987. The resulting reservoir is Choke Canyon Lake near the town of Cotulla, Texas. Austin, Texas, is located in the upper-left-hand corner of each image. Note the dramatic growth of the city, which has replaced farmland and grazing land.

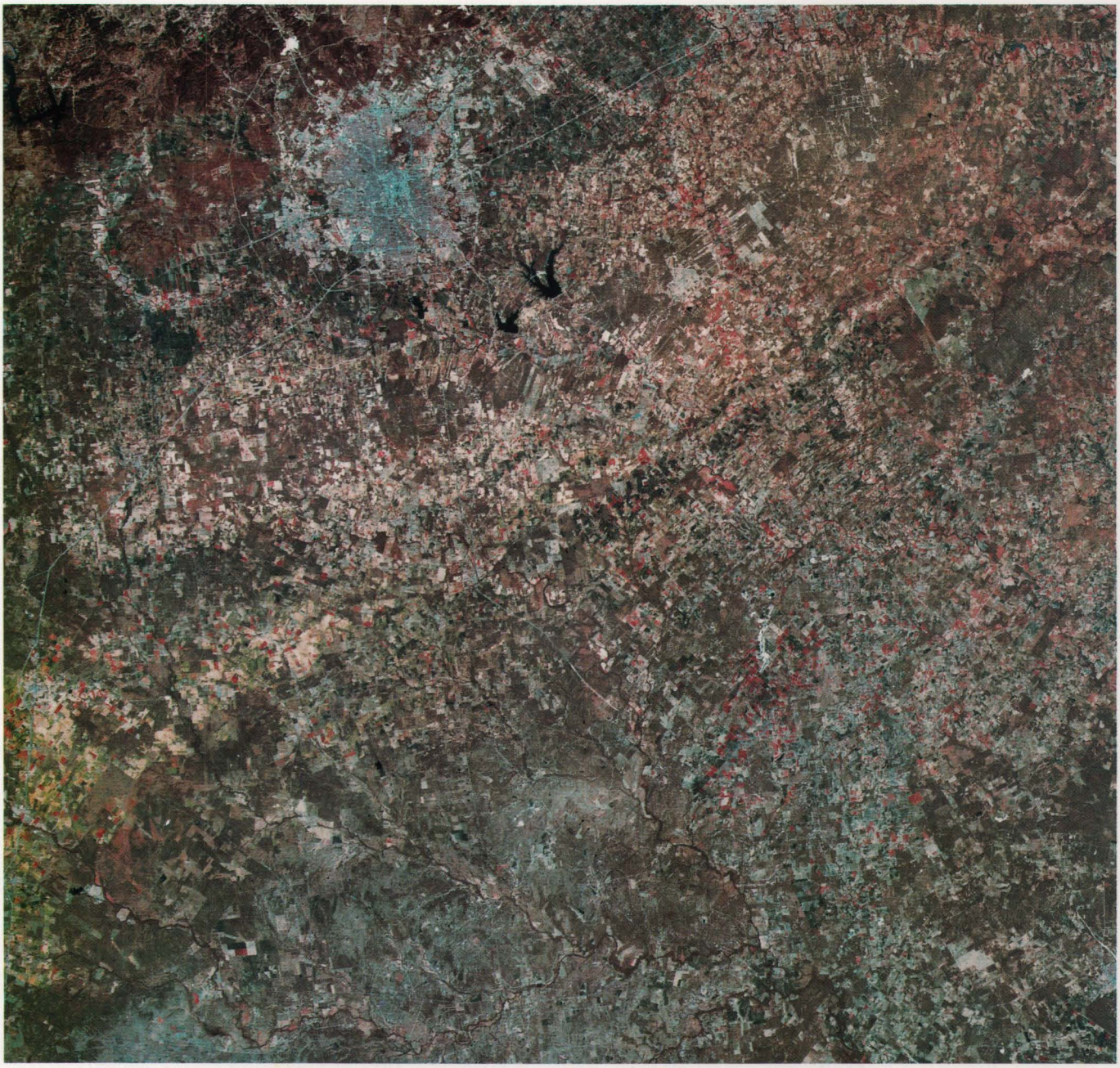

Landsat MSS
May 14, 1973

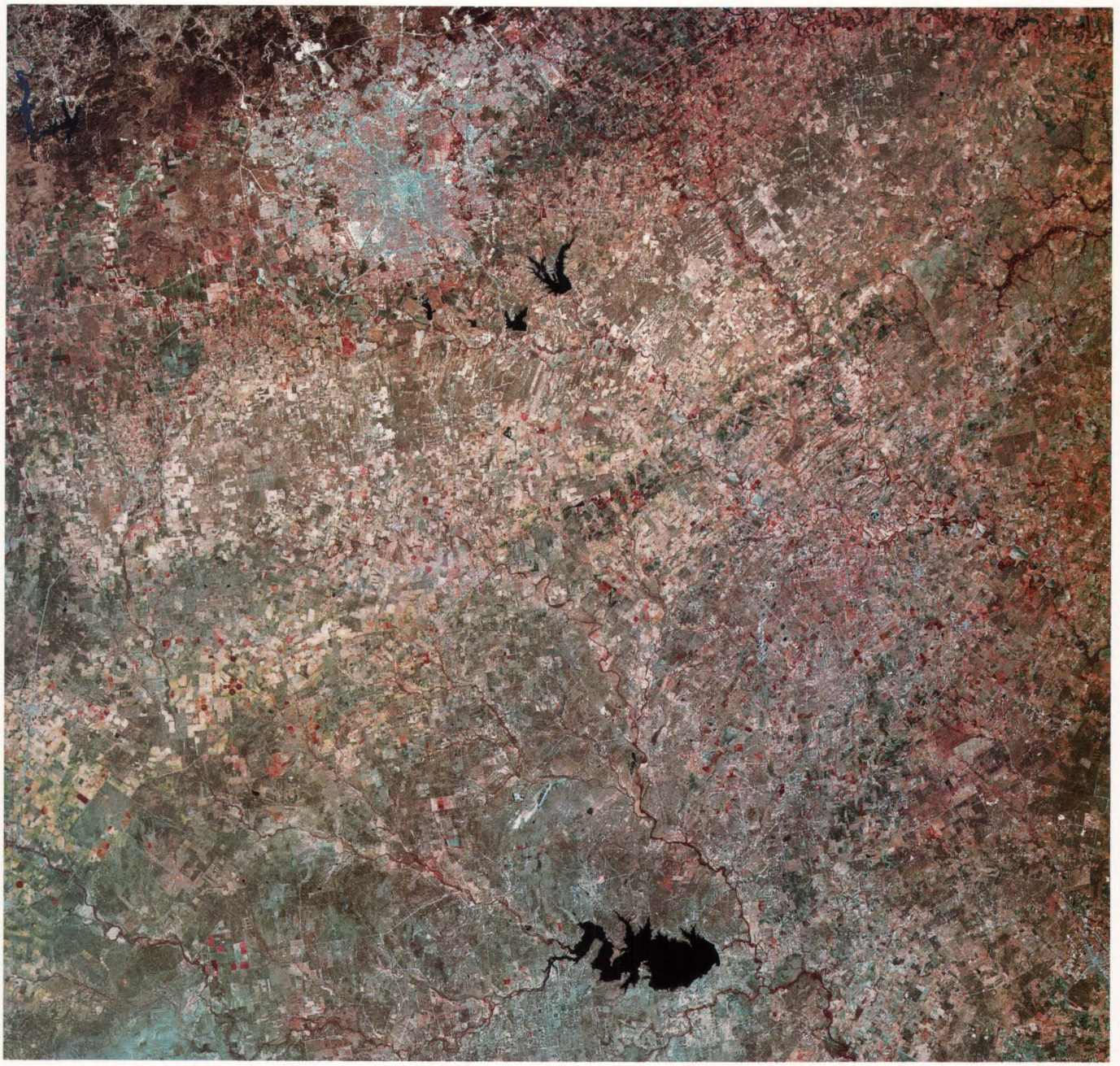

Landsat MSS
June 1, 1987

Lake Chad, Sahelian Region of West-Central Africa

Lake Chad, which forms part of the borders of Cameroon, Chad, Niger, and Nigeria, has decreased considerably since the 1960's because of prolonged drought. Early Gemini space photographs from the mid-1960's showed the lake basin full of water. The Landsat MSS image on December 8, 1972, shows the lake level lower than the mid-1960's level. In 1972, the lake area was approximately 25,000 km^2. After the extended drought of the 1970's and mid-1980's, the size of the lake shrunk to less than 2,000 km^2 (the light blue area at right-center in the October 14, 1987, image).

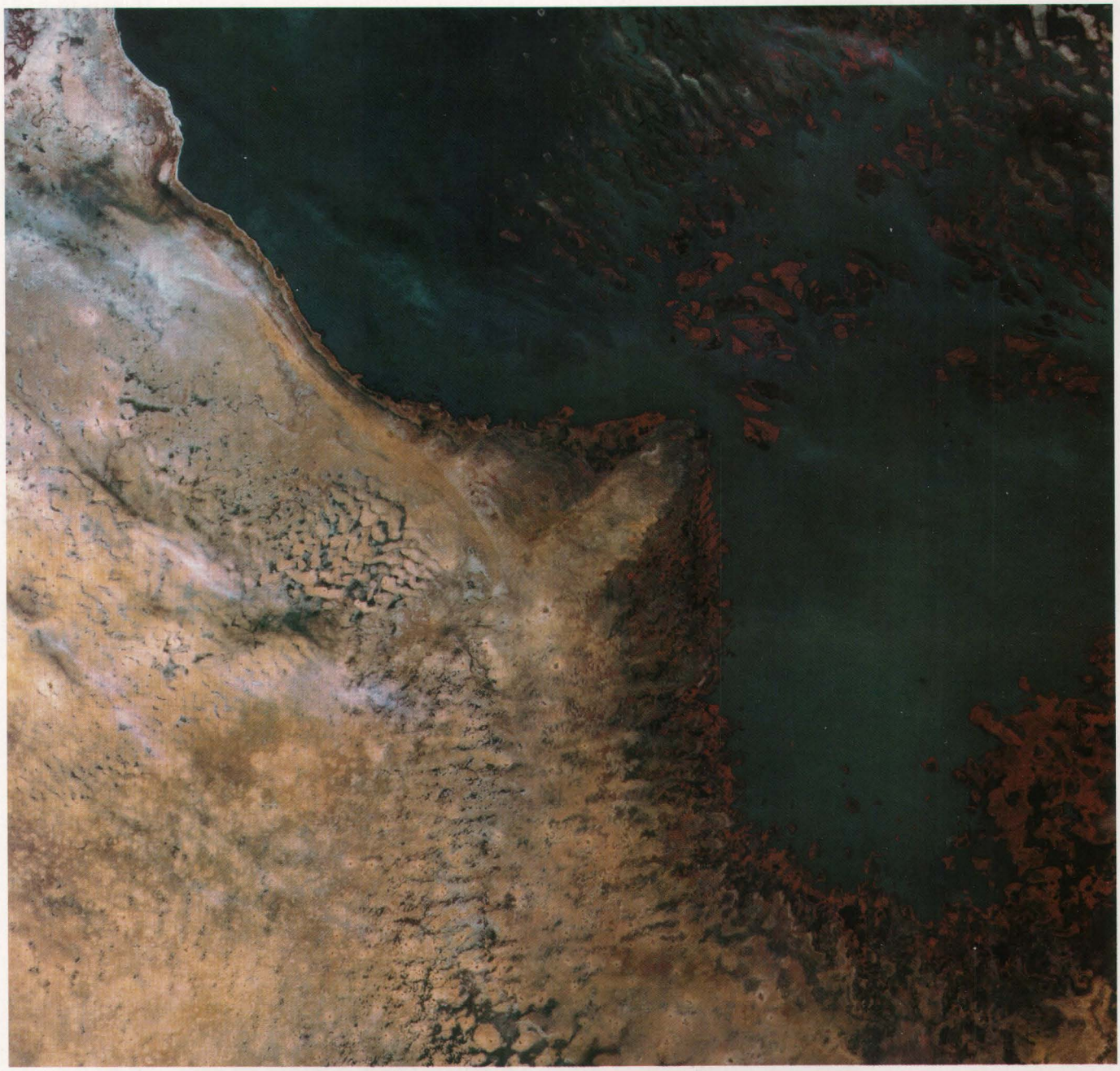

Landsat MSS
December 8, 1972

The Chari River, which provided about 80 percent of the total water supply for Lake Chad, was reduced to a trickle during the drought years. Many ancient dunes, long covered by the waters of the lake, are visible in the 1987 image. Note the old beach marks along the western side of the lake basin in 1987. The dark bluish-gray areas are dark hydromorphic soils. Much of the former lake has been replaced by marsh vegetation, indicating that the water table remains near the surface.

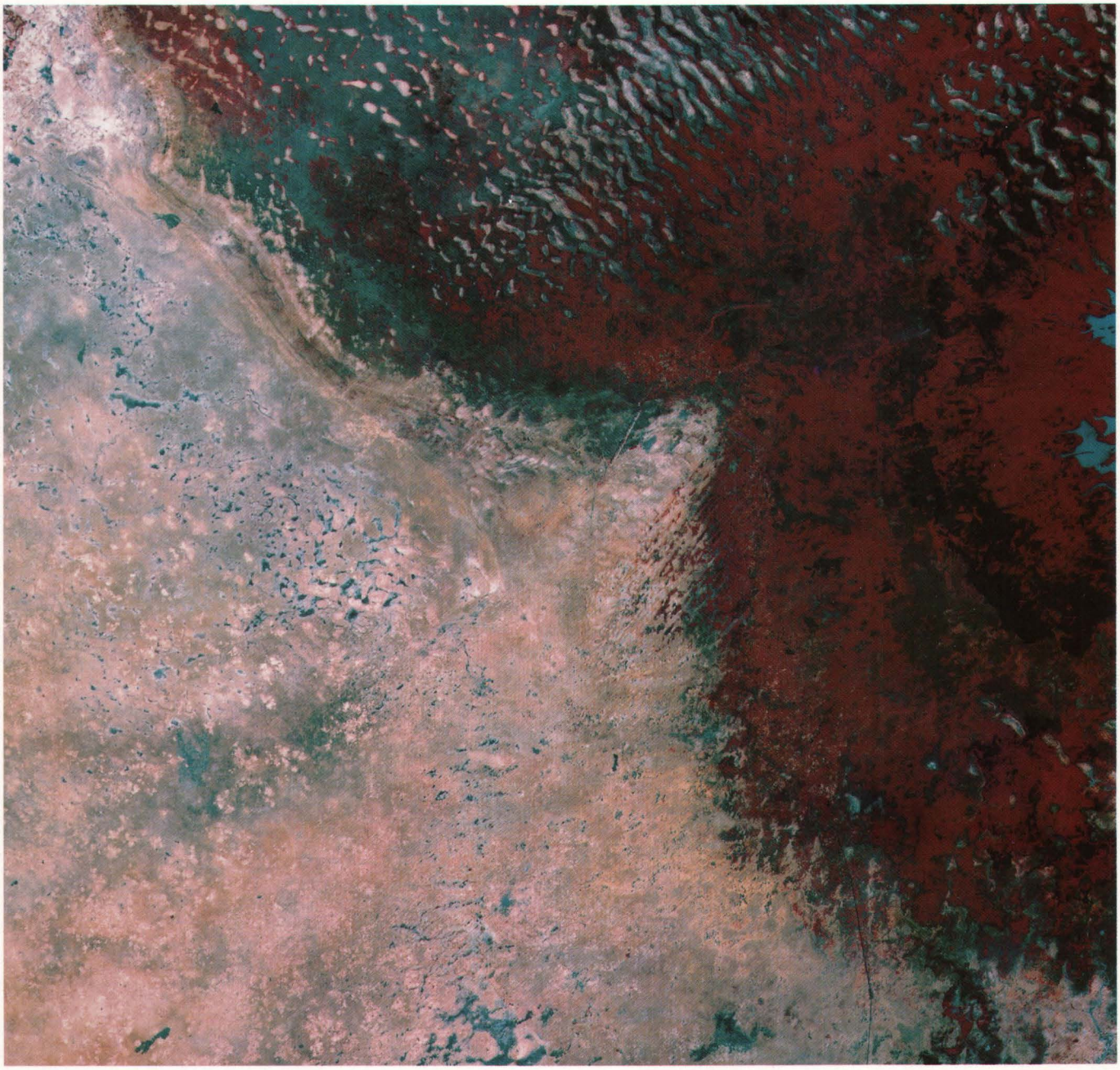

Landsat MSS
October 14, 1987

Aral Sea, Commonwealth of Independent States (formerly U.S.S.R.)

The receding shoreline of the Aral Sea is shown in the May 29, 1973, and August 19, 1987, Landsat images. In 1918, water began to be diverted from the two great rivers feeding the Aral, the Amu Darya and the Syr Darya, to irrigate millions of acres of land for cotton production. The waters from the two rivers now supply farms in Kazakhstan and Uzbekhistan, which produce 90 percent of the cotton grown in the Commonwealth. The inflow of water to the sea from these two rivers has been drastically reduced. From 1973 to 1987, the sea dropped from fourth to sixth among the world's largest lakes.

Landsat MSS
May 29, 1973

Environmental consequences of current practices include increased water salinity and significantly decreased biota in and on the shores of the sea. Huge storms of salt dust, originating from exposed sea bottoms, move with the prevailing winds. These storms deposit large amounts of salt on the land, up to 400 km from the Aral Sea, which affects crop growth in the area.

Landsat MSS
August 19, 1987

Zaliv Kara-Bogaz-Gol, Commonwealth of Independent States (formerly U.S.S.R.)

The depletion of water in the Zaliv Kara-Bogaz-Gol (KBG), an inlet bay on the eastern side of the Caspian Sea, is shown. By September 25, 1987, the Zaliv KBG was reduced to a small remnant, and the salinity jumped to 330 parts per thousand, making the bay poisonous to virtually all forms of life. The reduction of water in this bay is directly related to the diversion of water from the Ural, Volga, and Ehmba Rivers, which flow directly into the Caspian Sea. Also, in the mid-1970's, dams were built across the inlets between the Caspian Sea and the Zaliv KBG to reduce the loss of the Caspian Sea water by evaporation within the Zaliv KBG. This action further reduced the flow of water into the Zaliv KBG.

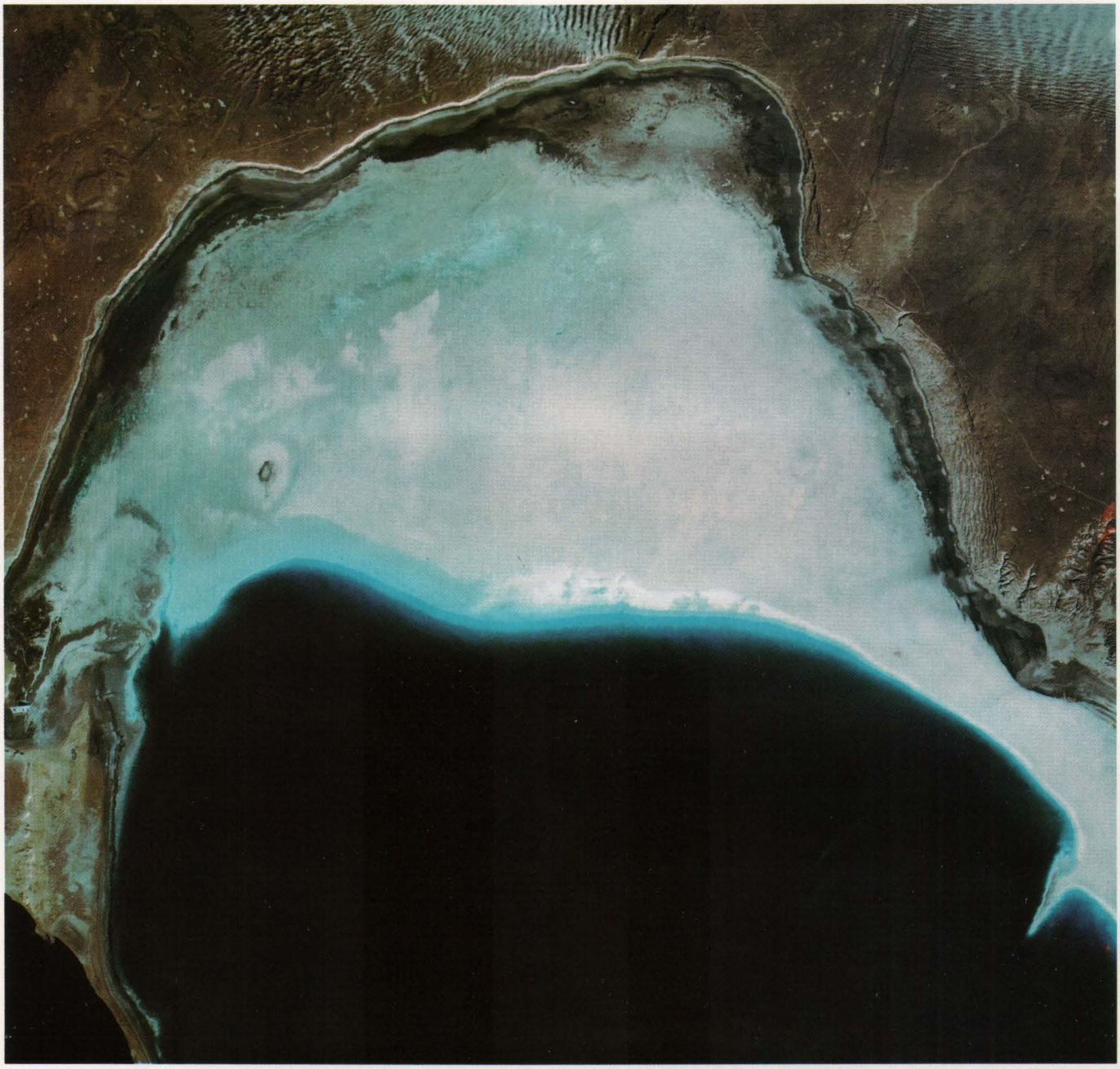

Landsat MSS
December 4, 1972

Landsat MSS
September 25, 1987

Lake Turkana, Ethiopia

Images from February 1, 1973, and January 12, 1989, show changes on the delta of the Omo River on the north shores of Lake Turkana in East Africa. The river delta has increased from 772 km^2 in 1965 to an estimated area of 1,800 km^2 in 1990. This 133-percent increase in delta area is the result of large-scale soil erosion in the watershed of the Omo River, which also has increased the turbidity within the lake. The erosion is directly related to grazing practices in the drainage basin of the Omo River and to a significant decrease in rainfall during the last 25 years. The reduction in rainfall also lowered the lake level, exposing additional land in the delta area of the lake.

Landsat MSS
February 1, 1973

Landsat MSS
January 12, 1989

Mississippi River Delta, Louisiana

Changes are shown in the Mississippi River Delta between January 16, 1973, and March 12 1989, by the vegetation (in shades of red) and sediment (aqua blue) at the mouth of the river. The increase in the land mass on the fringes of the delta and the decrease in land mass farther upstream within the delta, as seen on the 1989 image, can be explained by two factors: river channeling and increased turbidity. The Mississippi River has undergone major changes in recent years, one of which is the channeling of the river in the southern part of Louisiana. Levies and dikes were built to force the river to flow in its present course. This action reduces material deposits upstream and increases sediment deposits downstream on the fringes of the delta.

Landsat MSS
January 16, 1973

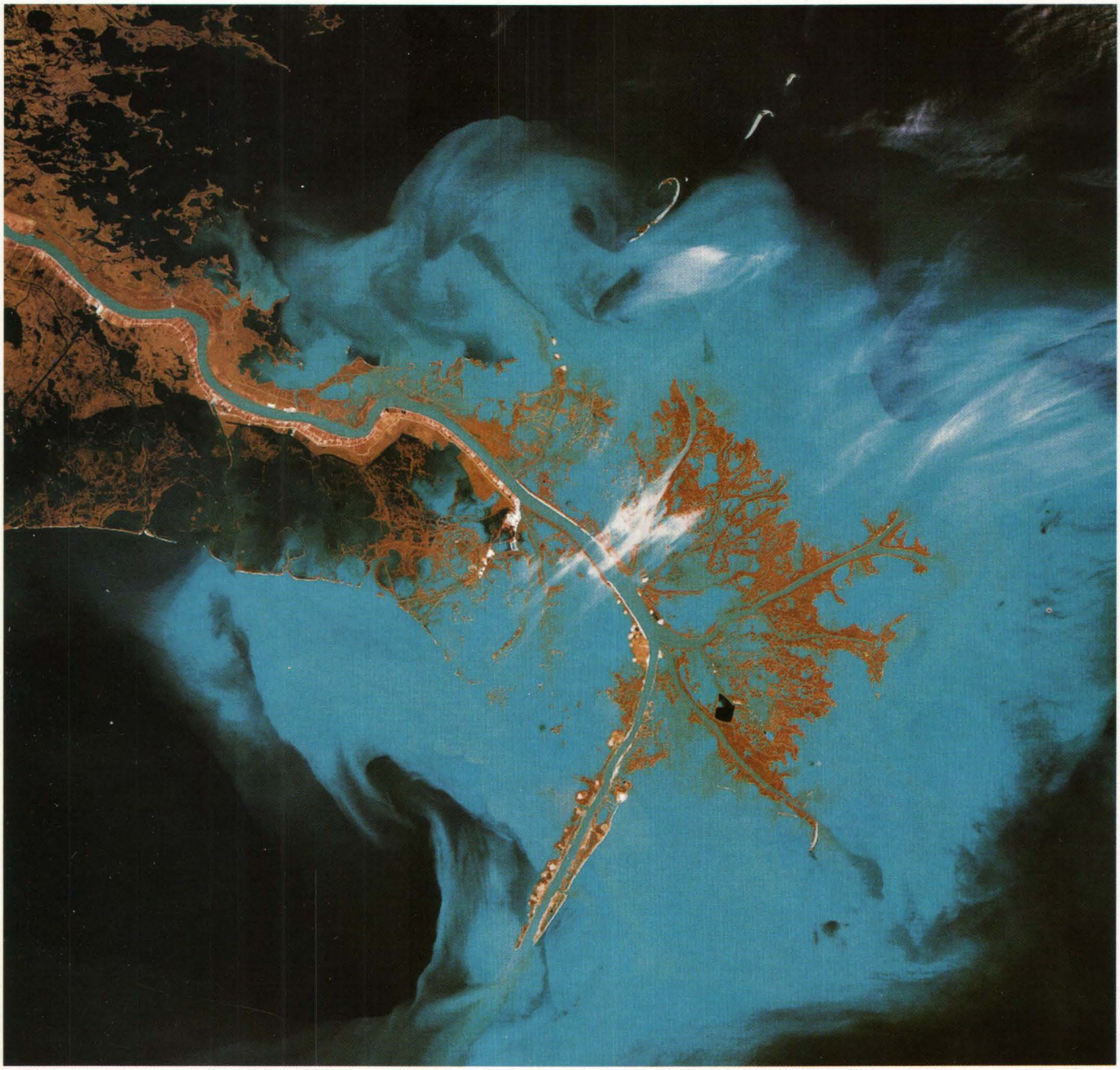

Landsat MSS
March 12, 1989

Great Salt Lake, Utah

The Landsat MSS images from 1972 and 1988 show the dramatic increase of the surface area of the Great Salt Lake in Utah. The rise in water level has increased the size of the lake to more than 966 km^2 and caused an estimated $200 million in damage by flooding highways, homes, and railways near the lake. In May 1986, the Utah legislature approved a project to pump excess water out of the Great Salt Lake onto a portion of the Bonneville salt flats west of the lake. This new water body, Newfoundland Evaporation Basin, which can be seen to the west of the Great Salt Lake in the 1987 image, was constructed to help control the level of the lake.

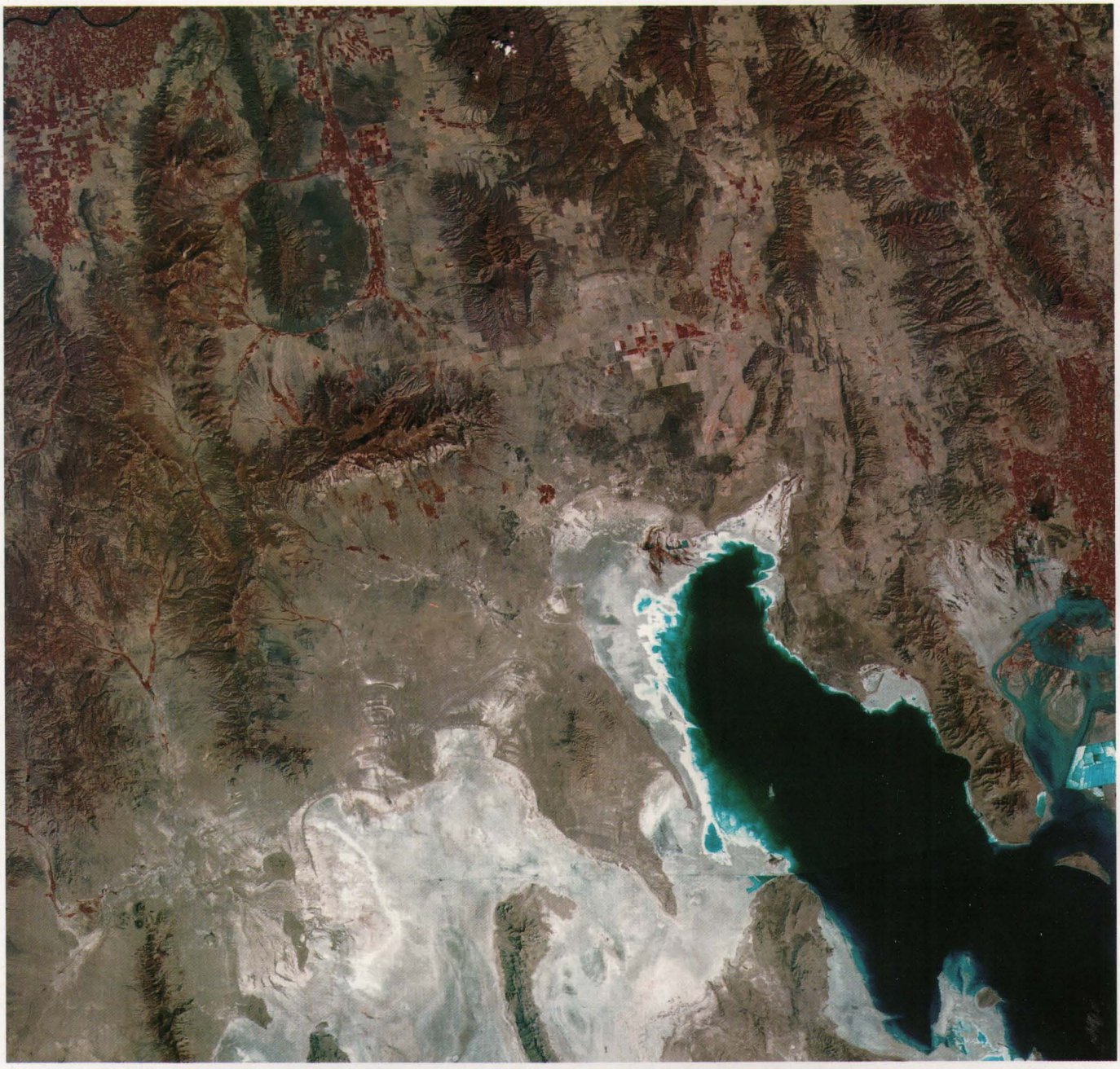

Landsat MSS
September 13, 1972

Landsat MSS
August 14, 1988

Accessing Landsat Data

The digital data and photographic products in this booklet and information on the availability of Landsat and other types of images can be obtained from the EROS Data Center.

Mail: U.S. Geological Survey
EROS Data Center
Customer Services Section
Sioux Falls, SD 57198

Telephone: (COMM): 605-594-6151
FAX - (COMM): 605-594-6589

Information on the availability of Landsat images can also be acquired through the Global Land Information System (GLIS), an interactive computer system developed by the USGS for accessing images and information on the EDC data archive. The GLIS provides scientists offline samples of earth science data that may be ordered through the system. Direct access to the GLIS is through wide-area networks and dial-up telecommunications interfaces. Contact the GLIS user assistance for more information on accessing the GLIS.

Mail: U.S. Geological Survey
EROS Data Center
GLIS User Assistance
Sioux Falls, SD 57198 USA

Telephone: 1-800-252-GLIS (1-800-252-4547)
(COMM): 605-594-6099

The Landsat images used in this booklet and their scene identification number and date of acquisition are listed below. The digital data are available on 6,250 BPI 9-track CCT and CD-ROM.

Description	Scene ID	Date
Lake Chad, West-Central Africa	8113808572500	December 8, 1972
Lake Chad, West-Central Africa	85132208514X0	October 14, 1987
Rondonia, Brazil	8214813385500	June 19, 1975
Rondonia, Brazil	85088313431X0	August 1, 1986
Aral Sea, CIS (formerly U.S.S.R.)	8131006183500	May 29, 1973
Aral Sea, CIS (formerly U.S.S.R.)	85126606125X0	August 19, 1987
Zaliv KBG, CIS (formerly U.S.S.R.)	8113406425500	December 4, 1972
Zaliv KBG, CIS (formerly U.S.S.R.)	85130306333X0	September 25, 1987
Nile River Delta, Egypt	8129108005500	May 10, 1973
Nile River Delta, Egypt	85123407551X0	July 18, 1987
Lake Turkana, Ethiopia	8119307221500	February 1, 1973
Lake Turkana, Ethiopia	84237207201X0	January 12, 1989
Northern Iran	8290406102500	July 14, 1977
Northern Iran	85129406410X0	September 16, 1987
Western Kansas	8102416511500	August 16, 1972
Western Kansas	85162816501X0	August 15, 1988
Mississippi River Delta, Louisiana	8117716023500	January 16, 1973
Mississippi River Delta, Louisiana	85183715554X0	March 12, 1989
Central Saudi Arabia	8115507042500	December 25, 1972
Central Saudi Arabia	85071606560X0	February 15, 1986
Dallas-Fort Worth, Texas	8159716305500	March 12, 1974
Dallas-Fort Worth, Texas	85184716310X0	March 22, 1989
South-Central Texas	8156116324500	May 14, 1973
South-Central Texas	85147916332X0	June 1, 1987

Description	Scene ID	Date
Great Salt Lake, Utah	8105217472500	September 13, 1972
Great Salt Lake, Utah	8516271744X0	August 14, 1988
Mount St. Helens, Washington	8141918253500	September 15, 1973
Mount St. Helens, Washington	84031018253X0	May 22, 1983
Mount St. Helens, Washington	8516441826 5X0	August 31, 1988
Yellowstone Nat. Park, Wyoming	8101517404500	August 4, 1972
Yellowstone Nat. Park, Wyoming *	y4257417403X0	August 2, 1989

*Landsat TM image - please call the EDC directly for ordering information because of restrictions on distribution.